MAY 30 1991

ORNL/TM-11541

ornl

ORNL
MASTER COPY

OAK RIDGE
NATIONAL
LABORATORY

MARTIN MARIETTA

Wallboard with Latent Heat Storage for Passive Solar Applications

R. J. Kedl

MANAGED BY
MARTIN MARIETTA ENERGY SYSTEMS, INC.
FOR THE UNITED STATES
DEPARTMENT OF ENERGY

ORNL/TM-11541
Distribution Category UC-202

Engineering Technology Division

WALLBOARD WITH LATENT HEAT STORAGE FOR PASSIVE SOLAR APPLICATIONS

R. J. Kedl

DATE PUBLISHED: May 1991

Prepared for
DOE Advanced Utility Concepts Division
under Interagency No. AL 10 01 00 0

Prepared by the
OAK RIDGE NATIONAL LABORATORY
Oak Ridge, Tennessee 37831-6285
managed by
MARTIN MARIETTA ENERGY SYSTEMS, INC.
for the
U.S. DEPARTMENT OF ENERGY
under contract DE-AC05-84OR21400

CONTENTS

	Page
ABSTRACT	1
1. INTRODUCTION	1
2. SCALE-UP OF IMMERSION PROCESS	5
3. THERMAL STABILITY TESTS	9
4. THERMAL PERFORMANCE	18
4.1 THERMAL CONDUCTIVITY AND THERMAL TRANSIENT DATA	23
4.2 CONFORMATION OF COMPUTER MODEL	25
5. SUMMARY AND CONCLUSION	40
REFERENCES	42

WALLBOARD WITH LATENT HEAT STORAGE FOR PASSIVE SOLAR APPLICATIONS

R. J. Kedl

ABSTRACT

Conventional wallboard impregnated with octadecane paraffin [melting point—23°C (73.5°F)] is being developed as a building material with latent heat storage for passive solar and other applications. Impregnation was accomplished simply by soaking the wallboard in molten wax. Concentrations of wax in the combined product as high as 35% by weight can be achieved. Scale-up of the soaking process, from small laboratory samples to full-sized 4- by 8-ft sheets, has been successfully accomplished. The required construction properties of wallboard are maintained after impregnation, that is, it can be painted and spackled. Long-term, high-temperature exposure tests and thermal cycling tests showed no tendency of the paraffin to migrate within the wallboard, and there was no deterioration of thermal energy storage capacity. In support of this concept, a computer model was developed to handle thermal transport and storage by a phase change material (PCM) dispersed in a porous media. The computer model was confirmed by comparison with known analytical solutions and also by comparison with temperatures measured in wallboard during an experimentally generated thermal transient. Agreement between the model and known solution was excellent. Agreement between the model and thermal transient was good, only after the model was modified to allow the PCM to melt over a temperature range, rather than at a specific melting point. When the melting characteristics of the PCM (melting point, melting range, and heat of fusion), as determined from a differential scanning calorimeter plot, were used in the model, agreement between the model and transient data was very good. The confirmed computer model may now be used in conjunction with a building heating and cooling code to evaluate design parameters and operational characteristics of latent heat storage wallboard for passive solar applications.

1. INTRODUCTION

Passive solar energy refers to a solar energy concept in which radiant energy is collected, stored, and released by natural means and does not involve mechanical devices such as pumps, blowers, storage vessels, and associated piping and ducting. A typical passive solar building may have large, south-facing, double- or triple-glazed windows to allow the solar radiation to enter the building and massive floors and walls to capture and store the radiation as heat. Subsequently, the floors and walls will release the stored heat as the occupied air space begins to cool. In this situation, thermal energy is stored as sensible heat, that is, the thermal energy storage (TES) is achieved by increasing the temperature of the storage media. A common occurrence with passive solar heated buildings is that the TES component (floor, walls) can overheat, and the occupied space becomes uncomfortable. A solution to this problem might be to reduce the size of the windows, but this would decrease the thermal performance of the passive solar system. However, to be cost effective, the thermal performance of the solar system must be as high as possible. The same logic also applies to other passive solar concepts such as Trombe walls and sun spaces. The common thread in all these applications is that the mechanism for TES is the sensible heat content of the massive storage medium.

An alternate mechanism for TES is to use the latent heat of fusion of a phase change material (PCM). Energy storage would be achieved by melting the PCM, and energy recovery would be achieved by freezing the PCM. Both energy storage and recovery take place at a constant temperature: the melting point of the PCM. Storage media with heats of fusion in the order of 232 kJ/kg (100 Btu/lb) are readily available [e.g., heat of fusion for ice water is 335 kJ/kg (144 Btu/lb)]. A pound of such material would require 105 kJ (100 Btu) to melt; this is a substantial amount of heat. Comparatively, one pound of brick, which has a heat capacity of 0.84 kJ/kg•°C (0.2 Btu/lb•°F), would have to increase in temperature by 278°C (500°F) to store the same amount of heat. The energy storage density obtainable with a PCM may be very high, and both energy storage and recovery take place at a constant temperature.

A PCM with a substantial heat of fusion and a melting point slightly above room temperature would be an ideal storage media for the passive solar application. The isothermal nature of the storage process could prevent overheating on a warm and sunny winter day. The high energy storage density could be used to convert low-mass building materials (e.g., wallboard) into materials with a high thermal mass. Other concerns are that the PCM must be chemically, physically, and biologically inert; stable; relatively cheap; and easily incorporated into conventional building materials.

Under Department of Energy (DOE) sponsorship, Dr. Ival Salyer of the University of Dayton Research Institute (UDRI) has identified the aliphatic paraffin series as an appropriate source of PCMs for this application. Background information on this concept is available in Refs. 1–6. The paraffins are stable and inert and have good thermal properties. Although any member of the paraffin series is suitable for TES, efforts were concentrated on octadecane, which has a melting point slightly above room temperature. Thermal properties of octadecane and its neighboring homologues are as follows:

	Melting point [C°(°F)]	**Heat of Fusion [kJ/kg (Btu/lb)]**
n-hexadecane ($C16H34$)	16.7 (62)	237 (102)
n-heptadecane ($C17H36$)	20.7 (69.3)	179 (77)
n-octadecane ($C18H38$)	26.6 (79.9)	246 (106)
n-nonadecane ($C19H40$)	30.4 (86.7)	182 (78)
n-eicosane ($C20H42$)	35.2 (95.3)	253 (109)

It has been demonstrated that the paraffins may be tailored by blending to obtain the desired melting point (Ref. 6). There are two commercial methods of manufacturing octadecane. First, octadecane may be prepared by an ethylene polymerization process. This method yields a purer material at a cost of \$3.30 to \$3.96/kg (\$1.50 to \$1.80/lb). The second process is based on the fractionation of petroleum refining residues. This method yields a less pure product, but at a cost of \$0.66 to \$1.10/kg (\$0.30 to \$0.50/lb).

UDRI selected conventional gypsum wallboard as the TES structural material of choice for its studies. The follwoing two methods were developed to incorporate paraffin into gypsum wallboard.

1. Wallboard immersed in molten octadecane will soak up the paraffin like a sponge. Simple immersion can yield a product containing up to 35% paraffin by weight of the composite. Higher concentrations may be obtained by exposing the wallboard to a vacuum before immersion and/or pressurizing the molten paraffin after immersion.
2. Solid pellets of cross-linked high-density polyethylene (HDPE) also absorb octadecane like a sponge. Exposing HDPE pellets to molten paraffin for 1 h at 80°C (175°F) results in a pellet that contains 80% paraffin by weight of the composite. These pellets can then be added to the mix of materials used in the manufacture of gypsum wallboard. Paraffin concentrations in wallboard product equivalent to the first method can be obtained.

Both methods of incorporating octadecane into wallboard are of commercial interest. The first method has the advantage that the paraffin may be added to fabricated wallboard and the wallboard manufacturer need not be involved. This method is of particular interest for concept development efforts because the researcher may prepare his own samples as required. The second method is of more interest to wallboard manufacturers because it involves less disruption to their manufacturing process. The pellets could be prepared elsewhere and simply added as another component to the gypsum mix used in the manufacture of wallboard.

The development of wallboard with latent heat storage includes a coordinated set of projects directed toward the ultimate commercialization of this product. These projects consist of

1. scale-up of the immersion process from small laboratory samples to full-sized sheets of wallboard [1.22 by 2.44 m (4 by 8 ft)];
2. demonstration of the physical and thermal stability of paraffin-impregnated wallboard, that is, showing that the paraffin does not migrate when thermally cycled and exposed to higher temperatures and that the storage capacity is maintained;
3. measurement of the thermal conductivity of wallboard impregnated with paraffin; and
4. development and validation of a computer model that will handle thermal transport and storage of a melting and freezing material.

These tasks are being addressed by Oak Ridge National Laboratory (ORNL) through the DOE-TES Program. This report will address the findings and current status of each of these tasks. Additional work is under way at (1) UDRI to investigate flammability and the effect of fire retardants on the flammability of wallboard impregnated with paraffin and (2) ORNL to model a passive solar building to determine the true thermal and cost effectiveness of these materials.

2. SCALE-UP OF IMMERSION PROCESS

The initial development work on this concept was conducted by UDRI, which typically worked with small-laboratory-size samples of wallboard, for example, 0.093 m^2 (1 ft^2) or less. As interest in the concept intensified, it became necessary to have a source of full-size sheets [1.22 by 2.44 m (4 by 8 ft)] of impregnated wallboard for experimental purposes. Because the immersion process is the most convenient, an effort was initiated at ORNL to prepare full-size sheets of wallboard impregnated with octadecane using this process. It was necessary to determine whether the amount of paraffin absorbed could be controlled and how uniformly it is distributed throughout the wallboard.

To accomplish this task, a heated pan large enough to accommodate a 1.22- by 2.44-m (4- by 8-ft) sheet of wallboard was fabricated and filled with molten octadecane paraffin. Wallboard was laid in a frame that featured a wire support bed for the wallboard. An overhead crane was used to immerse the frame and wallboard into the paraffin. Figure 1 shows a full-sized sheet being lowered into the paraffin. In these initial experiments, the

ORNL PHOTO 3551-90

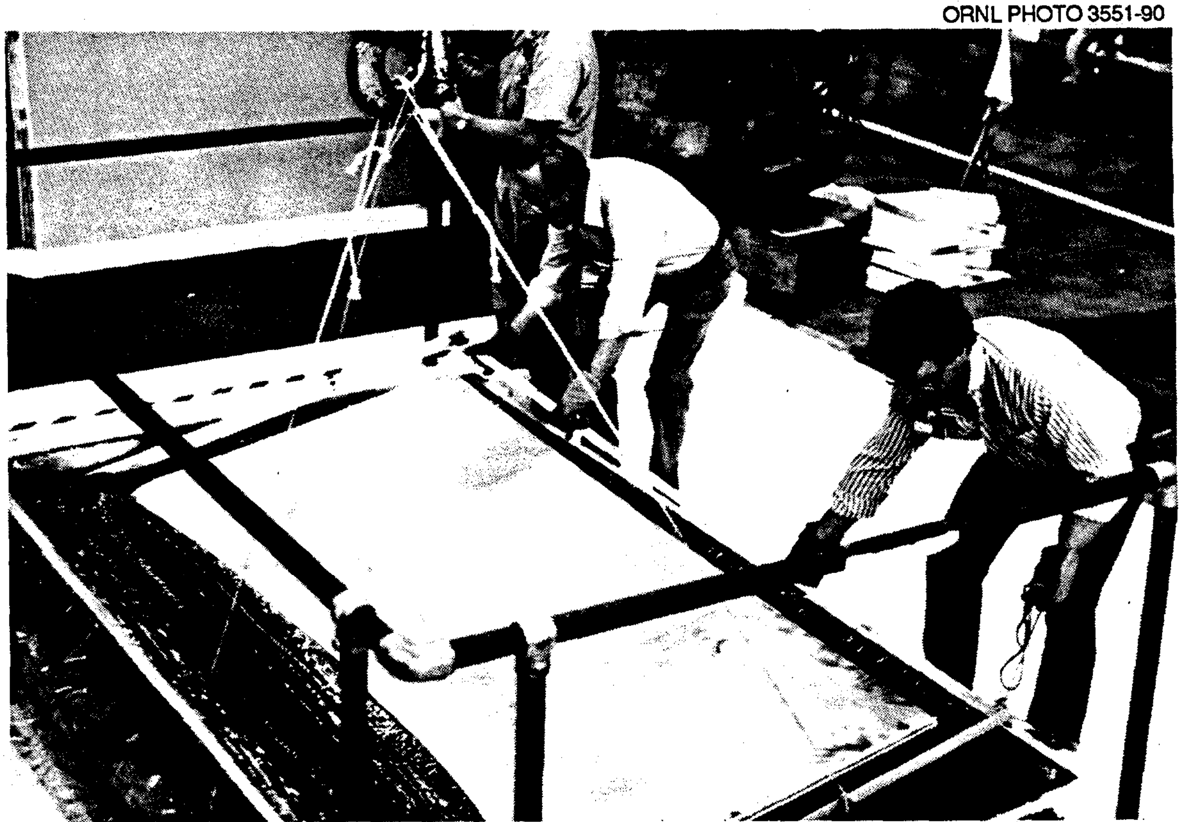

Fig. 1. Immersing wallboard in paraffin.

molten paraffin was maintained at 77°C (170°F). The paraffin was manufactured by the ethylene polymerization process and supplied by the Humphrey Chemical Company. The wallboard was supplied by the U.S. Gypsum Company in three thicknesses [0.64, 1.27, and 1.59 cm (1/4, 1/2, and 5/8 in.)] and came from the same manufacturing plant.

The immersion process was calibrated by dipping 0.30- by 0.30-m (1- by 1-ft) squares of wallboard into the paraffin bath for varying times and measuring the weight increase. These data are shown in Fig. 2, where the percent paraffin in the composite product is plotted against immersion time for all three thicknesses. Immersion time for the full-size sheets to reach the desired concentration was then determined from these plots; minimal adjustment time was necessary. Note that the 2.44-m (8-ft) edge of a sheet of wallboard is papered, but the 1.22-m (4-ft) edge is bare gypsum material. During immersion, air in the wallboard is displaced by paraffin and the air bubbles to the surface. Most of the air appeared to come from the unpapered 1.22-m (4-ft) edge, although a lot of air came from the 2.44-m (8-ft) papered edge. A small amount of air evolved from the flat surfaces as very small bubbles. It appeared that, during the soaking period, paraffin was being absorbed through the flat surfaces, displacing air, and forcing it out the edges. Note from Fig. 2 that the immersion times for full-size sheets are quite close to the immersion time for 0.093-m^2 (1-ft^2) samples to obtain a desired concentration. The significance is that the absorption rate per square foot of surface must be almost independent of size and that the edge effects must be minimal. This would seem to confirm this absorption mechanism.

The uniformity of paraffin distribution was demonstrated by the following experiment. A 1.22- by 1.22-m (4- by 4-ft) sheet of wallboard was immersed in paraffin long enough to result in a concentration of 25.7 wt % paraffin in the composite product. The sheet was then cut into 0.30- by 0.30-m (1- by 1-ft) squares by the scribe and break technique and each square weighed. Before immersion in the paraffin, each square would have weighed ~810 g. After immersion, the average weight of the squares was 1090 g with a standard deviation of only 12.1 g. Note that the scribe and break technique for cutting wallboard results in a jagged edge, but no material is lost as it would be from a saw blade kerf. The irregularities of the rough edge could account for some of the standard deviation. The conclusion is that octadecane paraffin distribution across the flat surface is quite uniform.

Red dye (Oil Red O) was added to the paraffin so that the wallboard could be broken and the penetration of the paraffin observed visually. Immediately after immersion, the paraffin was observed to be concentrated near the surfaces. However, if the wallboard was

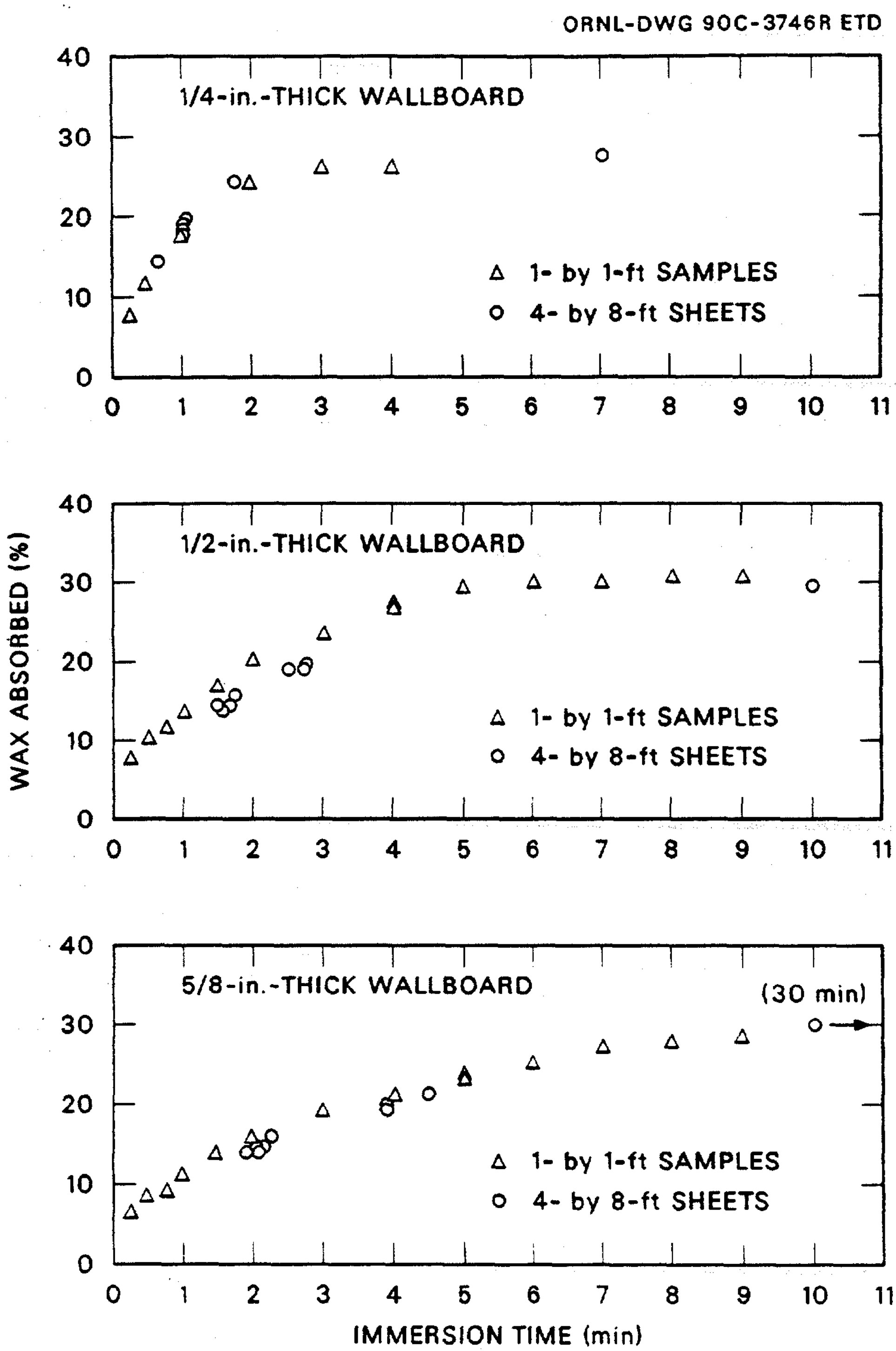

Fig. 2. Paraffin absorption by wallboard.

maintained at a temperature above the paraffin melting point for a period of time, the paraffin diffused, and the concentration became uniform across the thickness.

Having demonstrated that the amount of paraffin absorbed could be controlled by the immersion time and that the paraffin was uniformly distributed throughout the wallboard, some 50 full-size sheets were prepared. This production effort involved wallboard of three thicknesses (1/4, 1/2, and 5/8 in.) and three concentrations of paraffin in each thickness (15, 20, and 30% by weight). About half the sheets were sent to UDRI for thermal cycling and stability tests (discussed in Chap. 3), and about half were retained by ORNL for internal development activities (discussed in Chap. 4). Before these impregnated wallboards were used for any purposes, they were stored in an environmental chamber at 52°C (125°F) for one or more days.

Some time later, a second production effort resulted in the impregnation of an additional 110 full-size sheets of wallboard. In this case, the wallboard was supplied by the National Gypsum Company in two thicknesses (1/2 and 5/8 in.); the paraffin was supplied by the Witco Chemical Company, which manufactures paraffin by fractionation of petroleum refining residues. In this second production effort, the molten paraffin was maintained at 49°C (120°F) instead of 77°C (170°F). Fifty-three sheets of 1.27-cm (1/2-in.) wallboard were impregnated with 9.1 kg (20 lb) of paraffin each. This amount of paraffin gave the wallboards a latent heat storage capacity of 454 kJ/m^2 (40 Btu/ft^2) of surface. The 53 sheets were sent to the National Gypsum Company for internal studies directed toward assessing their commercial value. Fifty-six sheets of wallboard, involving both thicknesses, were impregnated to three concentrations of paraffin in each thickness (16, 20, and 30%). Most of the 56 sheets were sent to UDRI for flammability studies, but some were retained by ORNL for internal activities.

3. THERMAL STABILITY TESTS

Full-size sheets of wallboard impregnated with octadecane paraffin were tested for their thermal and physical stability at UDRI. The tests consisted of exposing impregnated wallboard to two kinds of thermal environments. In one test, several full-size boards were mounted vertically and exposed to a constant elevated temperature for an extended period of time. In the other test, several small samples of wallboard were thermally cycled above and below the octadecane melting point. Cycling was achieved by successively blowing warm air and cold air across the samples. Two kinds of cycling were involved. In cycle A, heating was achieved by blowing warm air on one side of the boards. Subsequently, cold air was blown across the other side of the board. In cycle B, warm and cold air were successively blown across the same side at the board. In all the tests described in this section, U.S. Gypsum wallboard impregnated with Humphrey Chemical Company technical grade octadecane paraffin was used. The purpose of these tests was to determine whether these thermal exposures will result in migration of paraffin or a deterioration of its thermal properties, and to assess the possibility of any problems. This research is described in detail in Ref. 7.

The high-temperature exposure facility is shown in Fig. 3(*a*) with the access door closed and in Fig. 3(*b*) with the access door removed. Edges of seven sheets of wallboard can be seen in the latter figure. The wallboards tested were all 1.27 cm thick (1/2 in.) and consisted of two samples each of three paraffin concentrations (nominally 30, 20, and 15%) and one control sample without paraffin. Before the test was started, three samples of impregnated wallboard were core drilled from each board for Differential Scanning Calorimeter (DSC) measurements. The thermal exposure test consisted of holding the seven full-size samples at 38°C ± 1°C (100°F ± 2°F) for a period of 3 months. Temperature was maintained by circulating warm air through the boards. The samples were visually inspected with a flashlight every day. The samples were weighed before the test and after each month during the exposure. At the end of the test, three more samples were core drilled from each sheet for DSC analysis.

The initial weight of the wallboards and the weight after each month are shown in Table 1. Note that in all cases the weight either decreased or remained the same as high-temperature exposure continued. The control experienced an initial weight loss of 57 g

ORNL PHOTO 3552-90

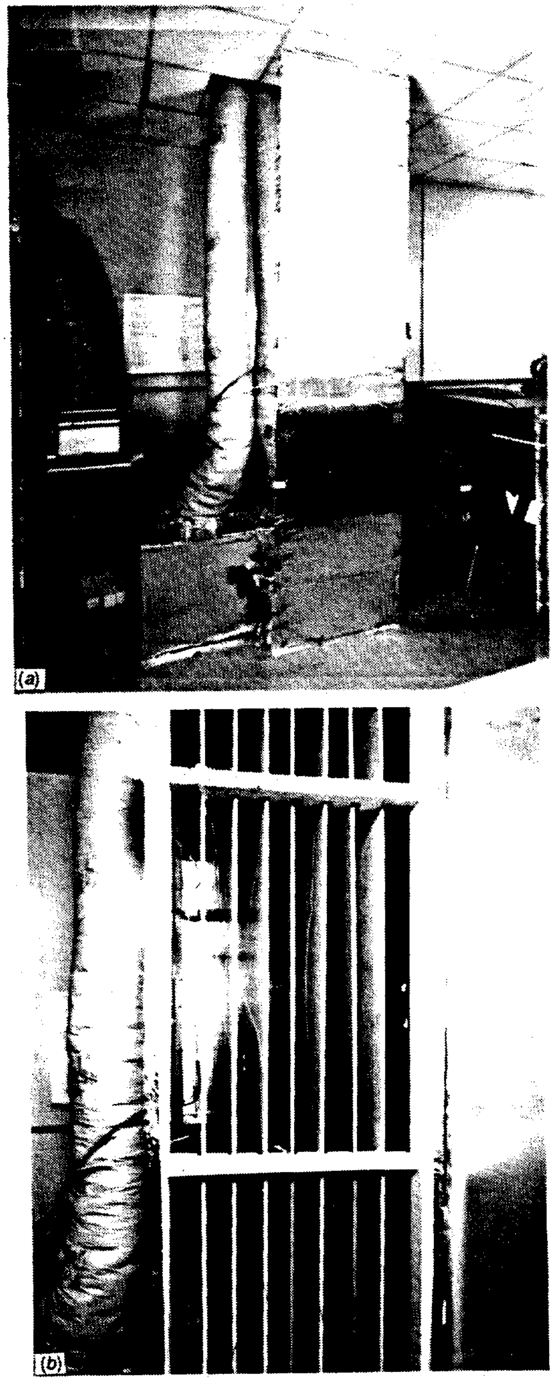

Fig. 3. High-temperature exposure facility with access door (*a*) closed and (*b*) open.

Table 1. Weight of wallboard initially and after each month of high-temperature exposure test

Board No.	PCM (%)	Initial weight (lb)	1 month (lb)	2 months (lb)	3 months (lb)
B1	29.8	83.0	83 7/8 (–1/8)	82 3/4 (–1/8)	82 1/2 (–1/4)
B2	30.0	81 13/16	81 5/8 (–3/16)	81 1/2 (–1/8)	81 1/4 (–1/4)
B8	19.6	71 7/16	71 1/4 (–3/16)	71 1/4, no change	71 (–1/4)
B9	20.2	71 3/4	71 1/2 (–1/4)	71 1/4 (–1/4)	71 (–1/4)
B12	15.0	67 1/4	67 (–1/4)	67, no change	66 3/4 (–1/4)
B13	14.7	68 1/4	67 7/8 (–3/8)	67 3/4 (–1/8)	67 1/2 (–1/4)
Control, 1/2 in.	0	58 1/4	58 1/8 (–1/8)	58 1/8, no change	58 1/8, no change
Average incremental weight loss of impregnated boards			1/4 lb or 113 g	1/8 lb or 57 g	1/4 lb or 113 g

(1/8 lb), then remained constant. This initial weight loss probably absorbed moisture. The impregnated boards continued to lose weight for the duration of the test.

This weight loss must result from evaporation of the paraffin. Based on the average monthly weight loss from Table 1 and accounting for about 1/8 lb of moisture in each board, the average evaporation rate is

$$\text{Evaporation rate} = \frac{(1/4 - 1/8) + 1/8 + 1/4}{3} = 77 \text{ g/month (0.17 lb/month) for a}$$

$$1.22\text{-} \times 2.44\text{-m } (4\text{-} \times 8\text{-ft}) \text{ sheet .}$$

Another indication of paraffin evaporation was that small, oily droplets were observed on the cooler hinges and door wall of the test chamber. DSC analysis confirmed that these oily droplets were octadecane paraffin. The evaporation of paraffin is not considered a serious problem for the TES wallboard concept for several reasons. In actual application, the exposed surfaces would normally be painted or covered with plastic or aluminum wall covering, thus impeding the evaporation. If evaporation is a concern, then the back surface could also be painted or covered. Secondly, the exposure temperature of 38°C (100°F) is considerably higher than the material would risk in actual application. Finally, UDRI has several small samples impregnated up to 30 wt % paraffin that have been stored in their laboratory for over 2 years; these have shown no measurable weight loss.

Detailed visual examination of the wallboards at the end of the test showed no other evidence of paraffin migration. For example, there was no evidence of paraffin accumulation at the bottom or near the edges of the wallboard.

DSC measurements of impregnated wallboard core samples were made before and after the high-temperature exposure test. The core samples were obtained with a 2.54-cm (1-in.) core drill. After removal of the cover paper, each sample was homogenized with a mortar and pestle and the DSC sample taken from the homogenized mix. The DSC was operated at a heating and cooling rate of 10°C/min (18°F/min). Each sample was cycled three times in the DSC, and the recorded parameter value was the average from the three cycles. Results of these tests showed expected experimental scatter in the heat of fusion measurements, but based on average valves, showed no signs of deterioration over the duration of the test.

The thermal cycling facility is shown in Fig. 4(*a*) with the access door closed and in Fig. 4(*b*) with the access door removed. In Fig. 4(*b*) the array of 0.093-m^2 (18.1 ft^2) samples used in this test may be seen. The sample identification and location in the array is shown in Table 2. Note that the array contains two samples of each of the paraffin concentrations for the 1.27- and 1.59-cm (1/2- and 5/8-in.) boards: one sample of each concentration for the 0.63-cm (1/4-in.) boards and one control sample (without paraffin) of each thickness. Note the three plugs in each sample. These are plugged core drilling holes for DSC samples.

Cycle A was conducted first. During this test the boards were heated by blowing warm air on one side and subsequently cooled by blowing cold air on the other side. The duration of one complete heating and cooling cycle was 4 h, so that six cycles were completed each day. During the heating cycle, warm air at 38 to 40°C (100 to 105°F) was used. At the

ORNL PHOTO 3553-90

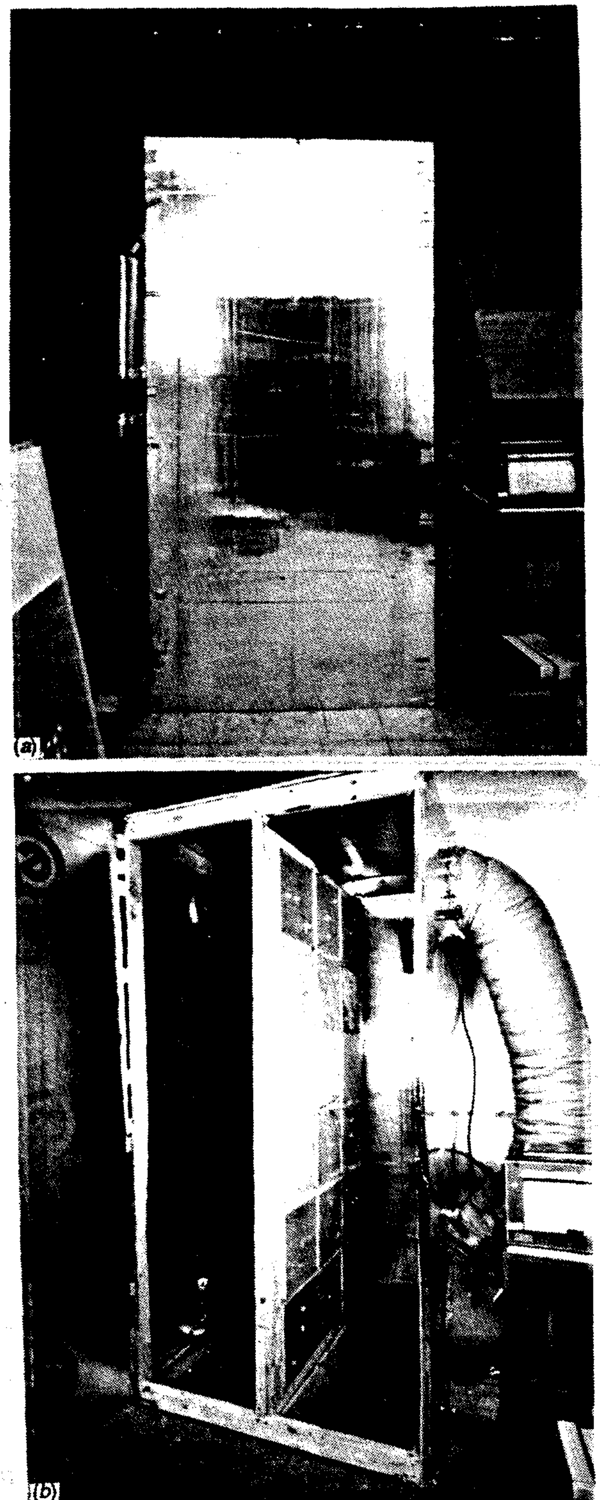

Fig. 4. Thermal cycling facility with access door (*a*) closed and (*b*) open.

Table 2. Sample identification and location in thermal cycling test

Sample A1 Thickness 0.63 cm (1/4 in.) 28.2% paraffin	Sample B14 Thickness 1.27 cm (1/2 in.) 14.9% paraffin	Sample C5 Thickness 1.59 cm (5/8 in.) 19.6% paraffin
Sample B6 Thickness 1.27 cm (1/2 in.) 19.4% paraffin	Sample C8 Thickness 1.59 cm (5/8 in.) 14.7% paraffin	Sample C1 Thickness 1.59 cm (5/8 in.) 30.6% paraffin
Control Thickness 0.63 cm (1/4 in.) No paraffin	Control Thickness 1.27 cm (1/2 in.) No paraffin	Control Thickness 1.59 cm (5/8 in.) No paraffin
Sample A7 Thickness 0.63 cm (1/4 in.) 14.9% paraffin	Sample B7 Thickness 1.27 cm (1/2 in.) 19.3% paraffin	Sample B15 Thickness 1.27 cm (1/2 in.) 14.4% paraffin
Sample C4 Thickness 1.59 cm (5/8 in.) 19.3% paraffin	Sample C9 Thickness 1.59 cm (5/8 in.) 14.7% paraffin	Sample B3 Thickness 1.27 cm (1/2 in.) 29.8% paraffin
Sample B4 Thickness 1.27 cm (1/2 in.) 30.6% paraffin	Sample A6 Thickness 0.63 cm (1/4 in.) 19.6% paraffin	Sample C2 Thickness 1.59 cm (5/8 in.) 30.4% paraffin

end of the heating cycle, the other side of the test fixture had reached 27 to 29°C (80 to 85°F). During the cooling cycle, cold air at –4 to +2°C (25 to 35°F) was used. At the end of the cooling cycle, the other side of the test fixture had reached 10 to 13°C (50 to 55°F). Thus, the paraffin was completely melted during the heating cycle and completely frozen during the cooling cycle. Visual observations were made each day during the test. The samples were cycled 200 times; thus, the test lasted about 34 d. At the end of the cycling test, the samples were removed and weighed. After weighing, a second set of core-drilled samples was taken for DSC measurements.

Cycle B was similar to cycle A except for the air flow technique for heating and cooling. The important difference between the two cycling techniques is that in cycle A, heat always flows in the same direction; whereas in cycle B, heat flows in one direction when the wallboard is heating and in the reverse direction when the wallboard is cooling. By comparing results of cycle A and cycle B, it should be possible to detect any thermally driven paraffin migration if any exists. As in the case of the A cycles, 200 heating and cooling cycles were completed and the same temperature limits were used. Visual observations were made each day and core drilled samples were taken at the end of the test for DSC measurements.

Weight loss from the wallboard samples during this test was found to be negligible for two reasons: (1) only one surface reached 38°C (100°F), and (2) this temperature was maintained for only a short period of time. By way of example, the evaporation rate measured during the high-temperature exposure test was about 0.17 lb/month [4 by 8 ft (both sides) at 100°F], [77 g/month – 1.22 by 2.44 m (both sides) at 38°C], which is equivalent to [0.04 g/d ft^2 (one side) at 100°F]. Each cycling experiment lasted about 34 d. During this period, one surface reached a temperature of 38°C (100°F) for a short period of time. For the purpose of calculation, we will assume that one surface was at or near 38°C (100°F) for a cumulative time of 10 d. Thus, the weight loss expected from paraffin evaporation would be (0.04) (10) = 0.4 g. This small weight loss is within the experimental scatter of the test.

DSC samples were handled the same way as in the high-temperature exposure test, and the results were similar. Although there was some experimental scatter in the heat of fusion, there was no indication of any deterioration or migration of the octadecane over the duration of the A cycle and B cycle tests.

An unexpected phenomenon was the appearance of paraffin frost on the cooler surface of the samples. Figure 5 is a photograph of the frost on sample C1 (30% paraffin). The frost seemed quite similar to hoarfrost that one sees on a cold winter morning. Figure 6 is a close-up photograph taken at ORNL. For perspective, the bottom half of the photograph represents a small area about 5 by 13 cm (2 by 5 in.) of the surface of a sheet of wallboard. A mechanical pencil is outlined with its point resting on the edge of the wallboard. It can be seen that the frost structures stand 0.25 cm (0.1 in.) high. During the A cycle tests, virtually all the panels developed some frost. Although highly visible, only a very small amount of paraffin was involved. Two of the panels were brushed and washed with methylene chloride. After this treatment the frost did not reappear. This observation leads to the belief that frosting is a phenomenon possibly related to oversaturation of the surface paper. Tests by UDRI show that acrylic latex paint stopped the frosting. It should be noted that frosting was considerably less with Witco paraffin (fractionated from petroleum residues) in National Gypsum wallboard than with Humphrey's paraffin (from ethylene polymerization) in U.S. Gypsum wallboard. Concerning the potential for paraffin-impregnated wallboard commercialization, frosting is considered to be a phenomenon for which a solution should be fairly easily and economically attainable.

ORNL PHOTO 3554-90

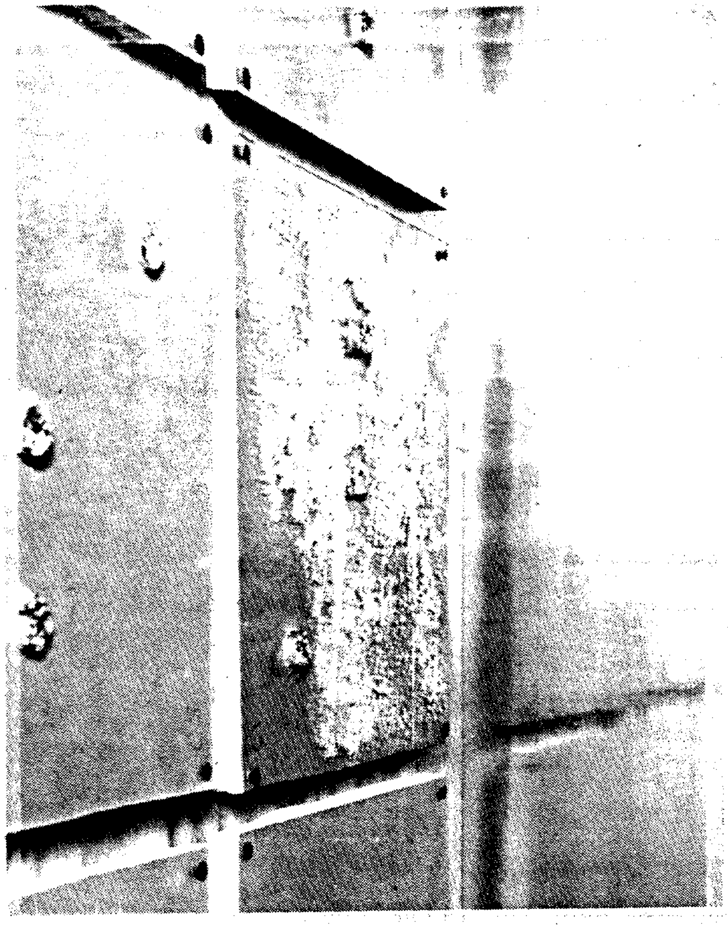

Fig. 5. Example of frosting in thermal cycling facility (sample C1, 30% paraffin).

ORNL PHOTO 8149-89

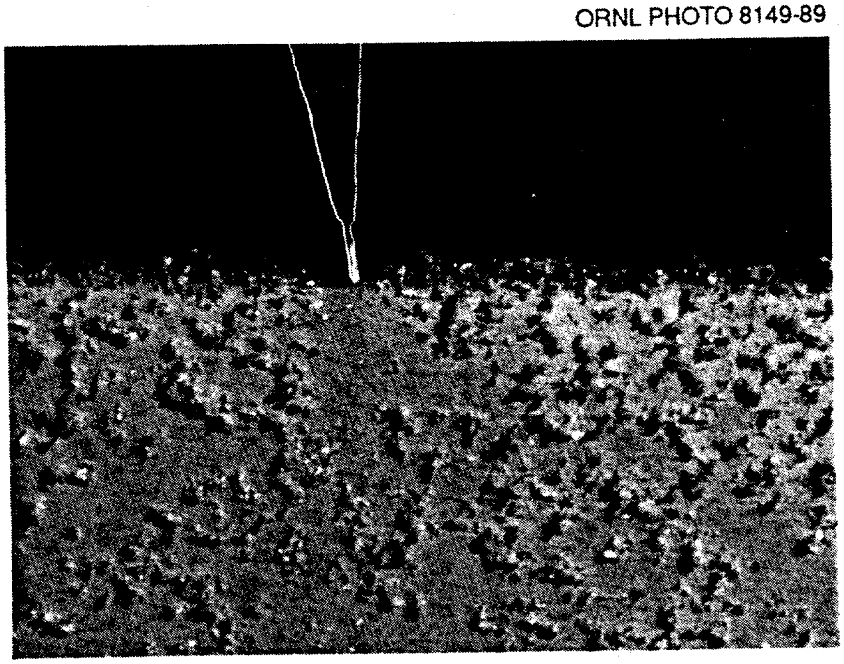

Fig. 6. Close-up view of paraffin frost.

Other than the frosting phenomenon, there were no other indications of paraffin migration in wallboard of any thickness or paraffin concentration observed during these cycling tests. In addition, there was no discernable difference in the paraffin behavior between A- and B-type cycles.

4. THERMAL PERFORMANCE

Considerable effort was directed toward determining and assessing the thermal performance of wallboard impregnated with octadecane paraffin. These efforts consisted of numerous DSC determinations by UDRI, measurements of thermal conductivity, and development and confirmation of a computer model that will accommodate thermal transport and storage of heat in a building material containing fixed PCMs. Ultimately the computer model will be incorporated into an existing building heating and cooling model, and the thermal performance of PCM-impregnated wallboard for the passive solar application will be determined.

Figures 7 to 10 show DSC results for the paraffins used in this program, and Table 3 summarizes the results for these plots. In most cases, two plots are shown: one with a 0.2°C/min (0.36°F/min) temperature ramp rate and the other with a 2.0°C/min (3.6°F/min) ramp. Because of thermal lag in the instrument, the measured melting temperature is always higher than the measured freezing temperature. This difference decreases as the temperature ramp decreases. Table 3 includes the average of the measured melting and freezing temperatures and is a good indication of the "handbook" melting point. Table 4 shows the distribution of n-decanes in the source material. Note that because the Humphrey Technical Grade octadecane is manufactured from polymerization of ethylene, its homologue contents are all numerically even. Because the Witco Technical Grade octadecane is manufactured by fractionation of petroleum residues, it contains all the homologues, but the amount peaks at C-18. Note that these concentrations are not necessarily for the material used in these tests but are representative of the technical-grade products.

The DSC plots in Fig. 7 are for the pure product. Figure 8 shows DSC plots for the Humphrey's octadecane. They both show a single melting temperature, but two freezing temperatures. Noteworthy is that the melting and freezing process occurs over a range of a few degrees Centigrade. Figure 9 shows DSC plots for the Witco octadecane. A second peak also shows up in this material, but it takes place at about 0°C (32°F) and may represent a solid-phase transition. Finally, Fig. 10 is a DSC plot of the material actually supplied to ORNL for these tests. The measured heat of fusion for all the technical-grade materials is about 20% lower than for the pure octadecane. The material used for these tests has a heat of fusion of about 45.6 cal/g, 82 Btu/lb, or 191 kJ/kg.

ORNL-DWG 90C-3747 ETD

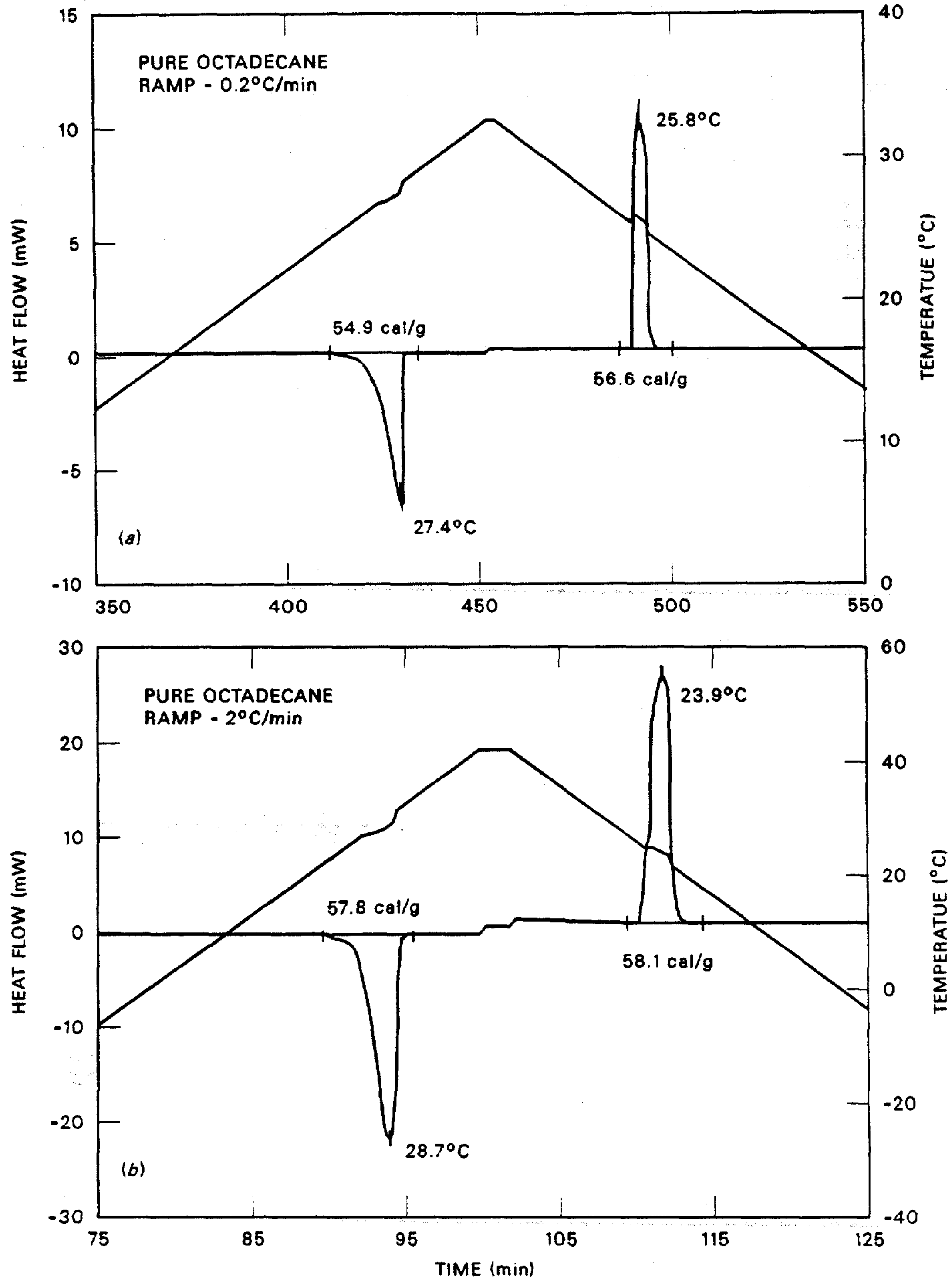

Fig. 7. DSC plot of pure octadecane at (*a*) 0.2°C/min and (*b*) 2°C/min.

ORNL-DWG 90C-3748 ETD

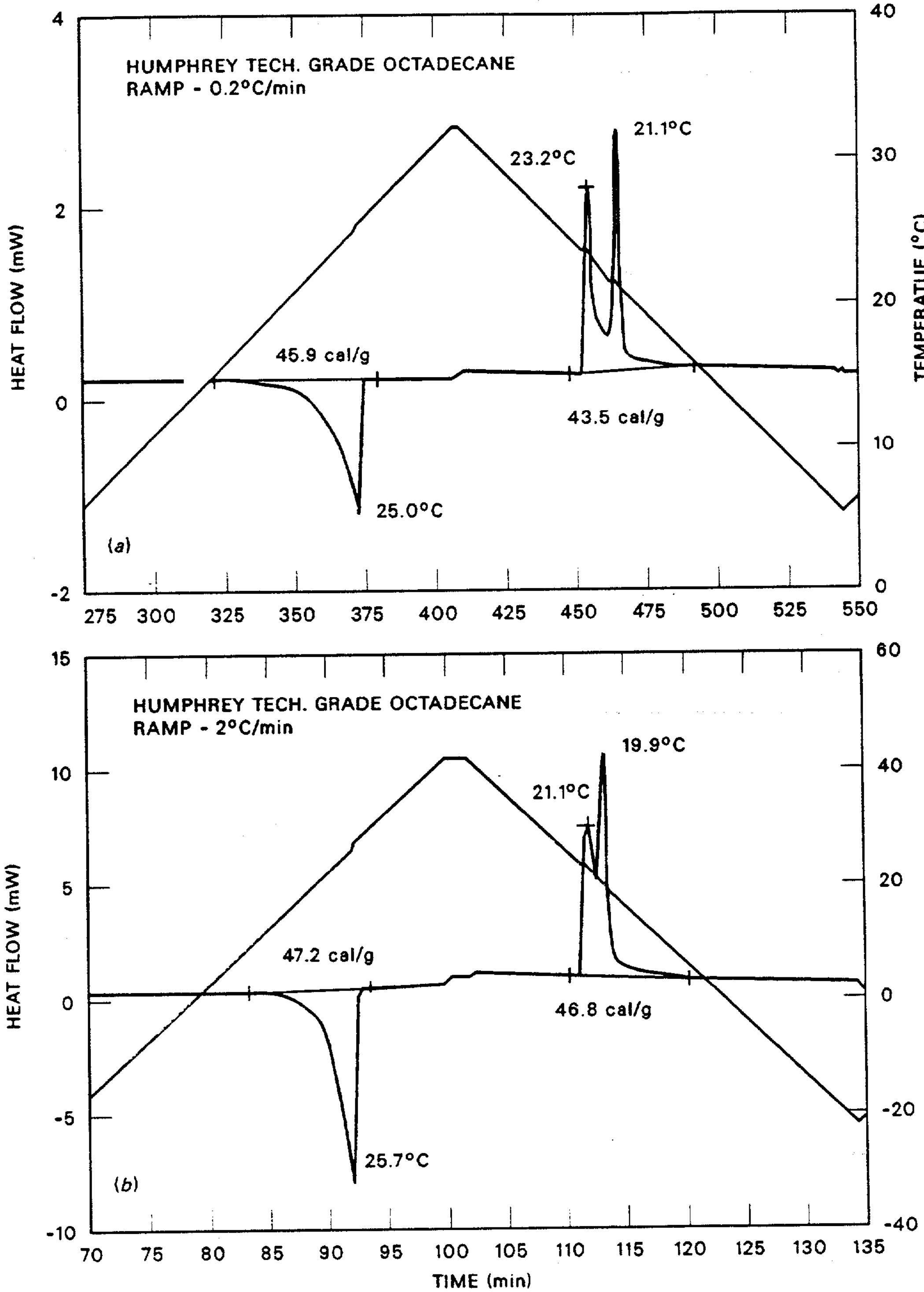

Fig. 8. DSC plot at pure Humphrey octadecane at (*a*) 0.2°C/min and (*b*) 2°C/min.

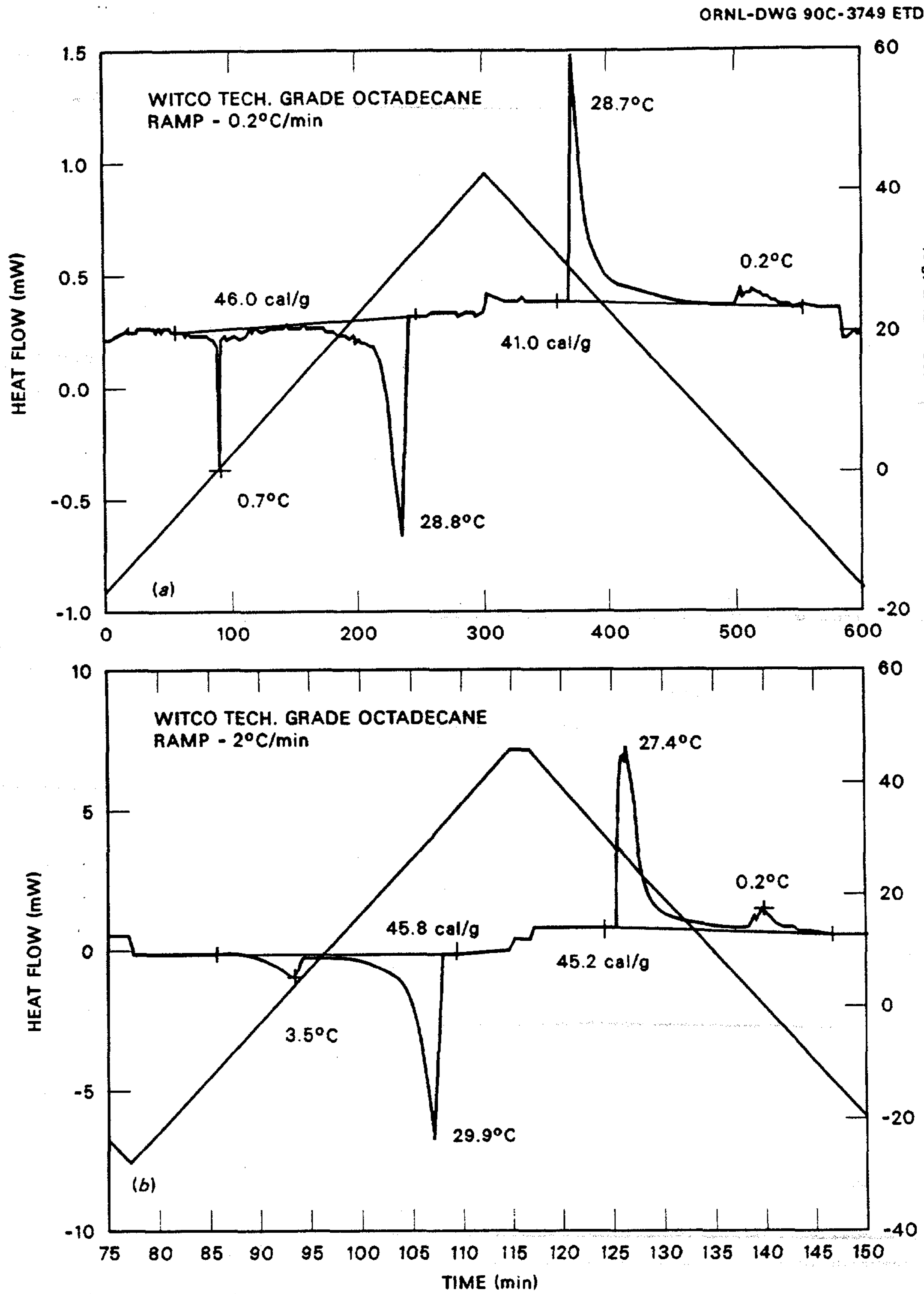

Fig. 9. DSC plot for Witco octadecane at (*a*) 0.2°C/min and (*b*) 2°C/min.

ORNL-DWG 90C-3750 ETD

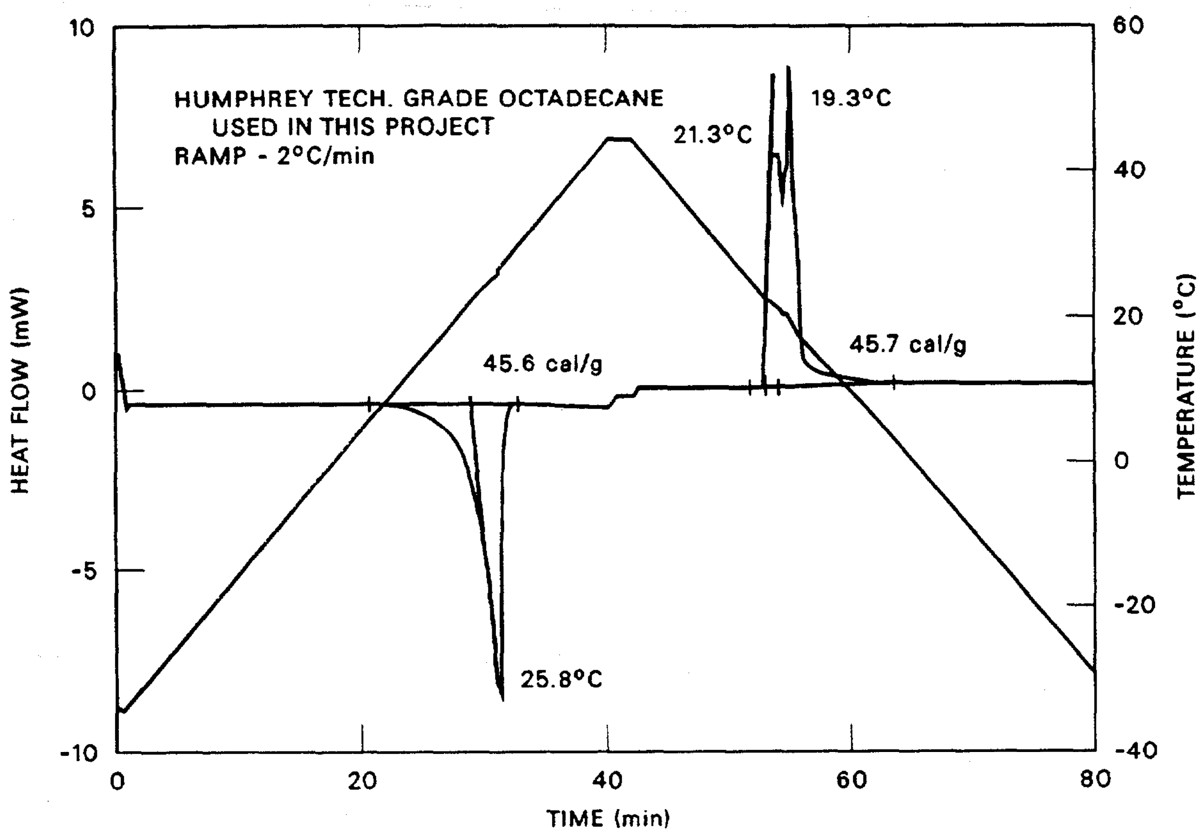

Fig. 10. DSC plot for the Humphrey octadecane, used in this project, at 2°C/min.

Table 3. Summary of DSC results for octadecane

Octadecane source	Ramp temperature (°C/min)	Temperature [°C (°F)]			ΔH fusion [cal/g (kJ/kg)]	ΔH crystal [cal/g (kJ/kg)]
		Melting	Freezing	Average		
Octadecane 99% pure	0.2	27.4 (81.3)	25.8 (78.4)	26.6 (79.9)	54.9 (230.0)	56.6 (237.2)
Octadecane 99% pure	2	28.7 (83.7)	23.9 (75.0)	26.3 (79.3)	57.8 (242.2)	58.1 (243.4)
Humphrey Tech grade	0.2	25.0 (77.0)	22.1 (71.8) (avg)	23.6 (74.4)	45.9 (192.3)	43.5 (182.3)
Humphrey Tech grade	2	25.7 (78.3)	21.0 (69.8) (avg)	23.4 (74.1)	47.2 (197.8)	46.8 (196.1)
Humphrey used in this effort	2	25.8 (78.4)	20.3 (68.5) (avg)	23.0 (73.5)	45.6 (191.1)	45.7 (191.5)
Witco Tech grade	0.2	28.8 (83.8)	28.7 (83.7)	28.7 (83.7)	46.0 (192.7)	41.0 (171.8)
Witco Tech grade	2	29.9 (85.8)	27.4 (81.3)	28.6 (83.5)	45.8 (191.9)	45.2 (189.4)

Table 4. Distribution of n-decanes in different sources

Octadecane source	C-14	C-16	C-17	C-18	C-19	C-20	C-21	C-22	C-24
Octadecane 99% pure				99.8		0.2			
Humphrey Tech grade	0.9	5.2		92.3				0.3	1.2
Witco Tech grade		8.2	25.1	26.3	20.5	10.1	3.6	1.0	

4.1 THERMAL CONDUCTIVITY AND THERMAL TRANSIENT DATA

The thermal conductivity of wallboard impregnated with paraffin was measured by an existing facility at ORNL that measures the conductivity of building materials. The facility, called the Unguarded Thin-Heater Apparatus (UTHA) (illustrated in Fig. 11), consists of a centrally located thin screen wire resistance heater with the building materials to be tested placed on both sides (two-directional heat flow) and enclosed (top and bottom) by thick copper plates containing cooling coils. The screen wire heater is rectangular and has dimensions of 0.91 by 1.53 m (3 by 5 ft). The sample to be tested is 0.61 by 0.91 m (2 by 3 ft) inside a "picture frame" of a material with a similar or lower thermal conductivity. The lateral area of the assembly is sufficiently large so that near the center of the assembly the heat flow is axial and edge effects may be neglected. Thus guard heaters are not required. The facility was built such that the minimum thickness that can be tested is ~3.8 cm (~1 1/2 in.). Therefore, when the 1.27-cm (0.5-in.) wallboard was tested, a stack of four sheets was required above and below the screen wire heater.

The thermal conductivity of wallboard containing 0, 15, and 30% paraffin (U.S. Gypsum Wallboard and Humphrey Chemical Company paraffin) was measured. The measurements were made with 1.27-cm (0.5-in.) wallboard; the results are shown in Fig. 12 (Ref. 8). Note that the thermal conductivity of the composite is 3 to 5% less when the paraffin is molten than when it is frozen. The UTHA was also used to generate experimental thermal transient data that were used to confirm the computer model. The procedure was as follows: first, the stack of eight sample sheets of wallboard (four above and four below the heater) was allowed to become isothermal at a temperature below the melting point of the paraffin. During this period the heater was turned off and the temperature of the wallboard stack was controlled by the cooling coils. Thermocouples were placed on the heater, between each sheet of wallboard, and between the wallboard and copper cooling plate. Five

ORNL–DWG 86-13967A

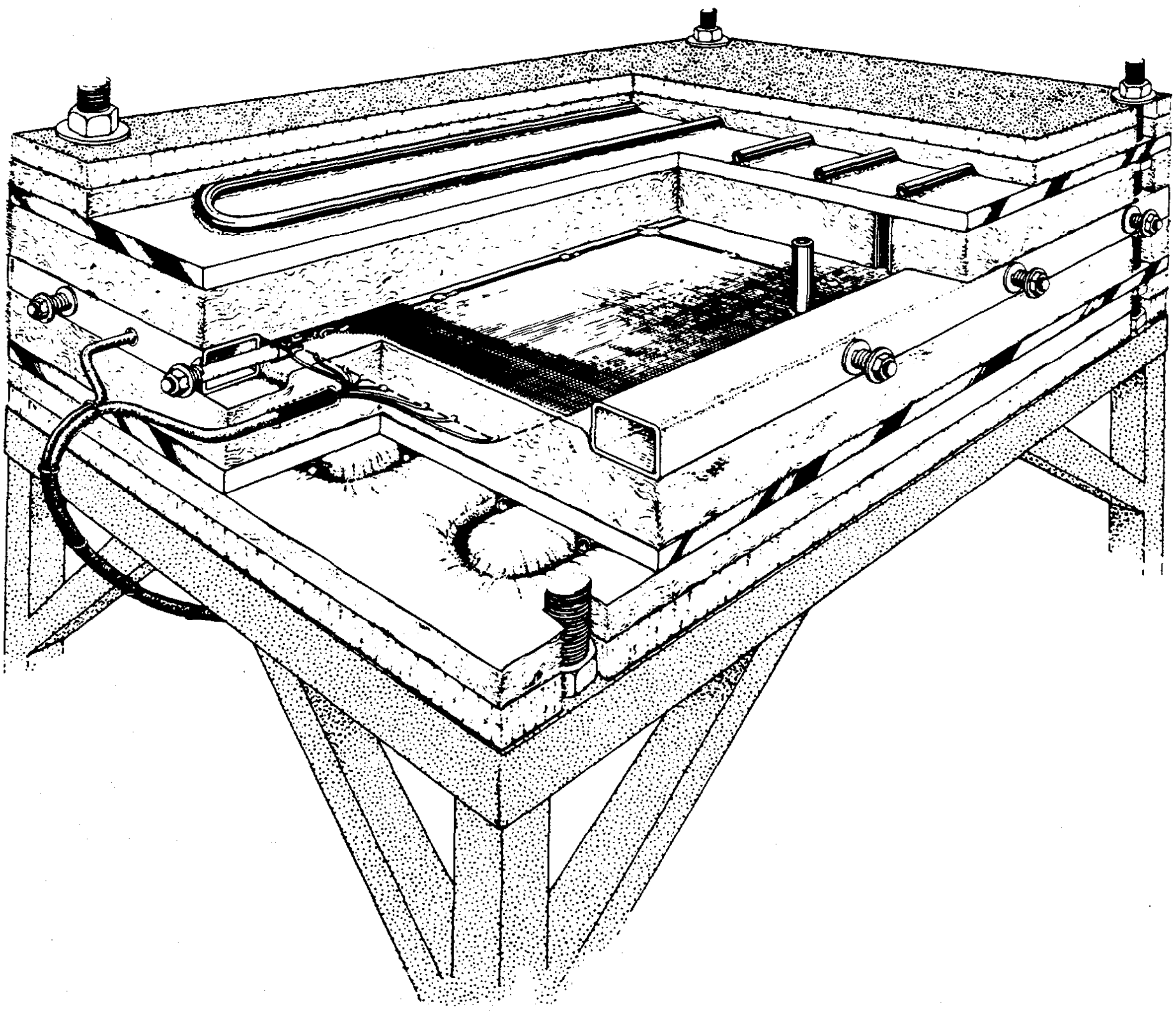

Fig. 11. Unguarded Thin-Heater Apparatus (UTHA) for measursing thermal conductivity.

thermocouples were located at each position. Typically, several days were required for the stack to become isothermal. At time equal to zero, the heater was turned on to some predetermined power level, and the thermal transient was initiated. The heater power level and the copper plate temperature were held constant, and all temperatures were recorded continuously during the transient. Typically a transient lasted several days. At the end of the transient, the temperature gradient through the stack of wallboard was a straight line. Thus knowing the heater power and the temperature difference across the stack, the thermal conductivity used in the computer model confirmation studies could be computed. Note that the copper cold-plates were maintained below the melting point during the entire transient,

ORNL-DWG 91M-2829 ETD

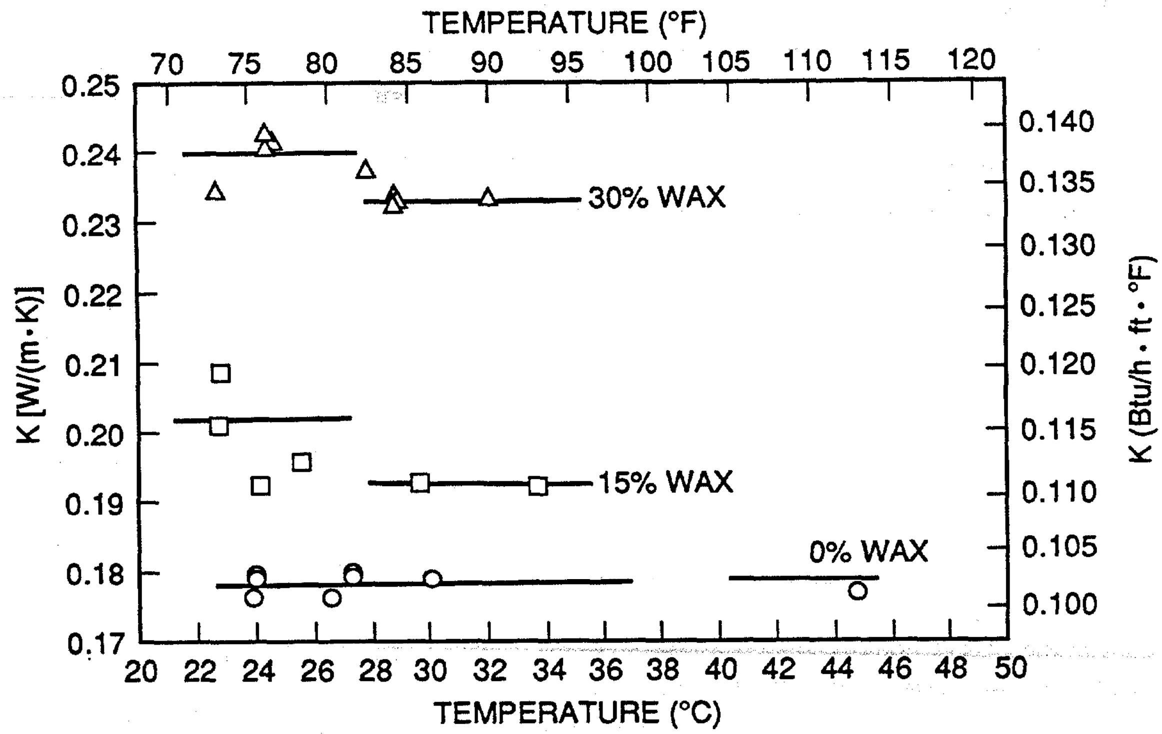

Fig. 12. Thermal conductivity of wallboard impregnated with octadecane paraffin.

but the wallboards near the heater were taken above the melting point. At the end of the transient, the liquid–solid phase front was located somewhere inside the stack.

4.2 CONFIRMATION OF COMPUTER MODEL

WALL88 is a numerical code developed to handle transient thermal transport and storage of both sensible and latent heat in multicomponent building materials. Specifically, WALL88 was prepared for the two-dimensional (2-D) rectangular case of wallboard. The code can treat the PCM as if it were uniformly mixed with the matrix material or as if the PCM were present in the form of discrete 2-D pellets distributed randomly throughout the solid support matrix. The randomness of the method is based on the use of a random number generator. The surface boundary condition considers both convective heat transfer to the room air and direct gain of solar energy. A constant surface temperature can also be imposed by setting the heat transfer coefficient to be very high. The mathematical foundation for the code is discussed in Ref. 9. WALL88 is available on diskettes in source and executable forms, in FORTRAN and Microsoft BASIC language versions.[10] Confirmation of the model consisted of verifying the operation of both its sensible heat and latent heat components.

Most of the transient tests were conducted with wallboard containing 30% paraffin. Recall that a transient starts with all the sheets of wallboard isothermal, at a temperature determined by the cold plates, and the heater off. Figure 13 shows a side-view schematic of the UTHA and defines the temperature locations. At time equal to zero the heater is turned on, but the cold plates continue to maintain the upper and lower temperatures constant. Figure 14 shows the results of such a transient. Note that the initial temperature of this transient is 26.5°C (79.7°F), which is above the melting point of the paraffin. Thus the paraffin is all molten, and sensible heat is the only thermal storage mechanism involved. The electrical heater power level generated a heat flux of 84.5 kJ/h•m^2 (7.45 Btu/h•ft^2) in each direction (up and down). Knowing the heat flux, the temperature difference between the heater [31.7°C (89.0°F)] and the cold plate [26.5°C (79.7°F)], and the thickness [5 cm (2 in.)], the overall thermal conductivity was calculated to be 0.835 kJ/h•m•°C (0.134 Btu/hr•ft•°F). Based on this conductivity, WALL88 was used to compute the transient; these results are also shown in Fig. 14. In this calculation, the heat capacity was taken to be 1.47 kJ/kg•°C (0.35 Btu/lb•°F). Note that the agreement between measured and computed values is very good for temperature locations T_H and T_3 but deviates for temperature locations T_1 and T_2. This is caused by variations in individual properties of the four layers of wallboard. If, for example, the thermal conductivity used in the calculation was computed based on the measured temperature difference between T_c and T_1, then the computed and measured values

ORNL-DWG 90-3751R ETD

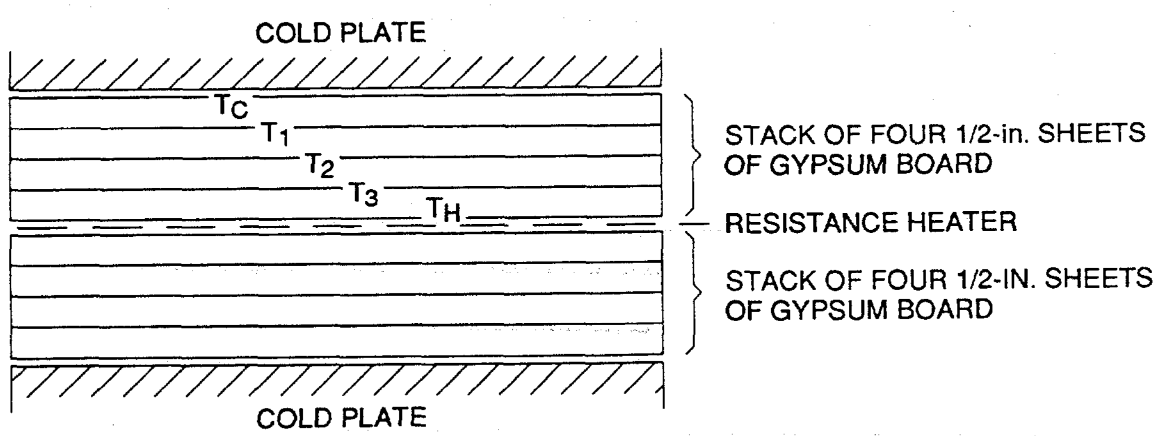

Fig. 13. Schematic of UTHA defining thermocouple locations.

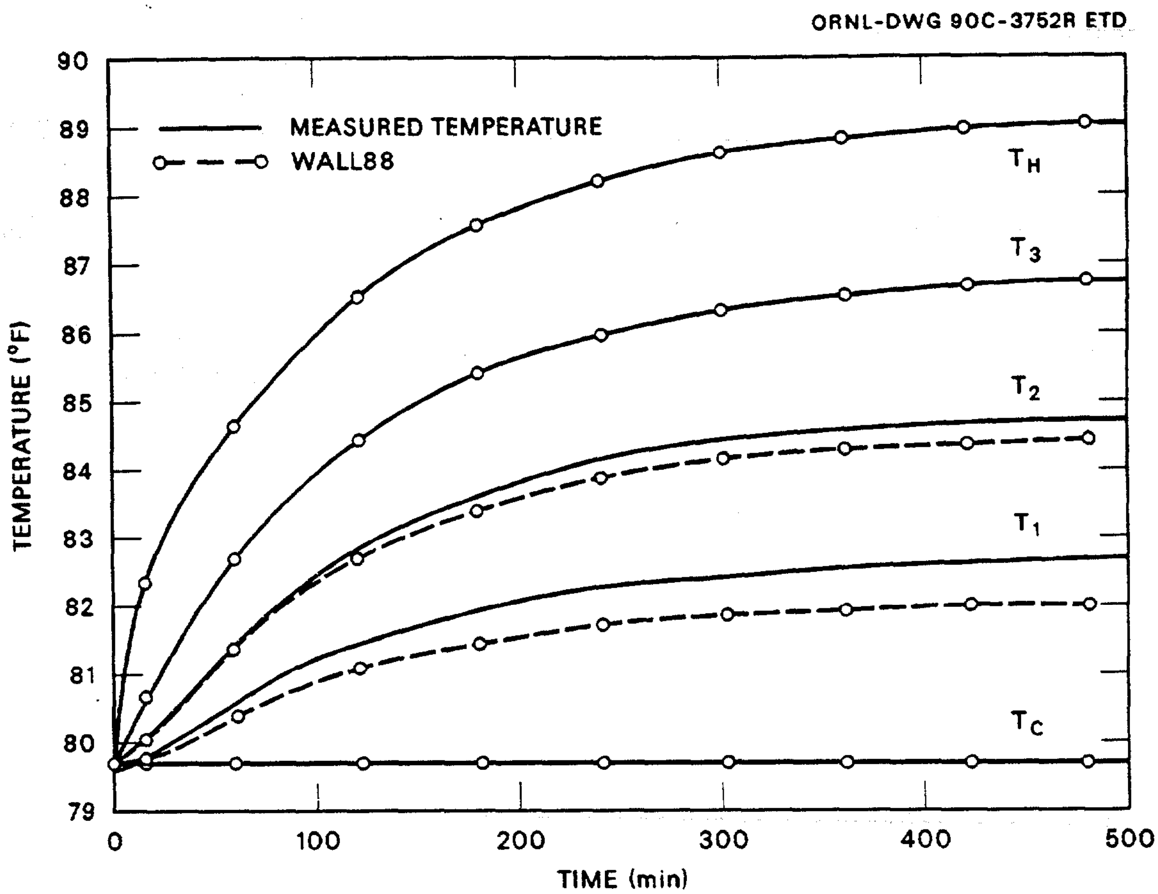

Fig. 14. Comparison of WALL88 with experimental transient. Heat capacity is only energy storage parameter involved.

of T_1 would be in good agreement; however, the predictions of T_H would be inaccurate. Based on these results, it was concluded that the ability of WALL88 to handle sensible heat transients has been verified.

The capability of WALL88 to accommodate latent heat was verified by comparing its results to a known analytical solution.[11] The physical situation for which a solution is known is a semiinfinite volume of immobile liquid at its melting point. At time equal to zero, the surface of the semiinfinite solid is fixed at a temperature below the melting point, and the liquid starts to freeze. The derived equation relates the temperature in the solid phase to distance and time. For this calculation we have taken the liquid to be initially at −6.7°C (20°F), which is also its melting point. At time equal to zero the surface was fixed at −17.78°C (0°F). Other parameters are heat capacity = 1.47 kJ/kg•°C (0.35 Btu/lb•°F), conductivity = 0.835 kJ/h•m•°C (0.134 Btu/h•ft•°F), density = 1.0 g/cm^3 (62.4 lb/ft^3), and heat of fusion = 58.8 kJ/kg (25.3 Btu/lb). The temperature profile in the solid was then computed after 4 h; results are shown in Fig. 15. The agreement is quite good, and it was concluded that the ability of WALL88 to predict temperature response for this case has been verified.

Nevertheless, it was believed that the best confirmation of WALL88 would result from its comparison with an experimentally produced transient. Thus, the transient with wallboard containing 30% paraffin was repeated. At this occurrence, the initial temperature was 22.5°C (72.5°F), which is below the melting point of about 23.0°C (73.5°F) (see Table 3). A lower

ORNL-DWG 90C-3753 ETD

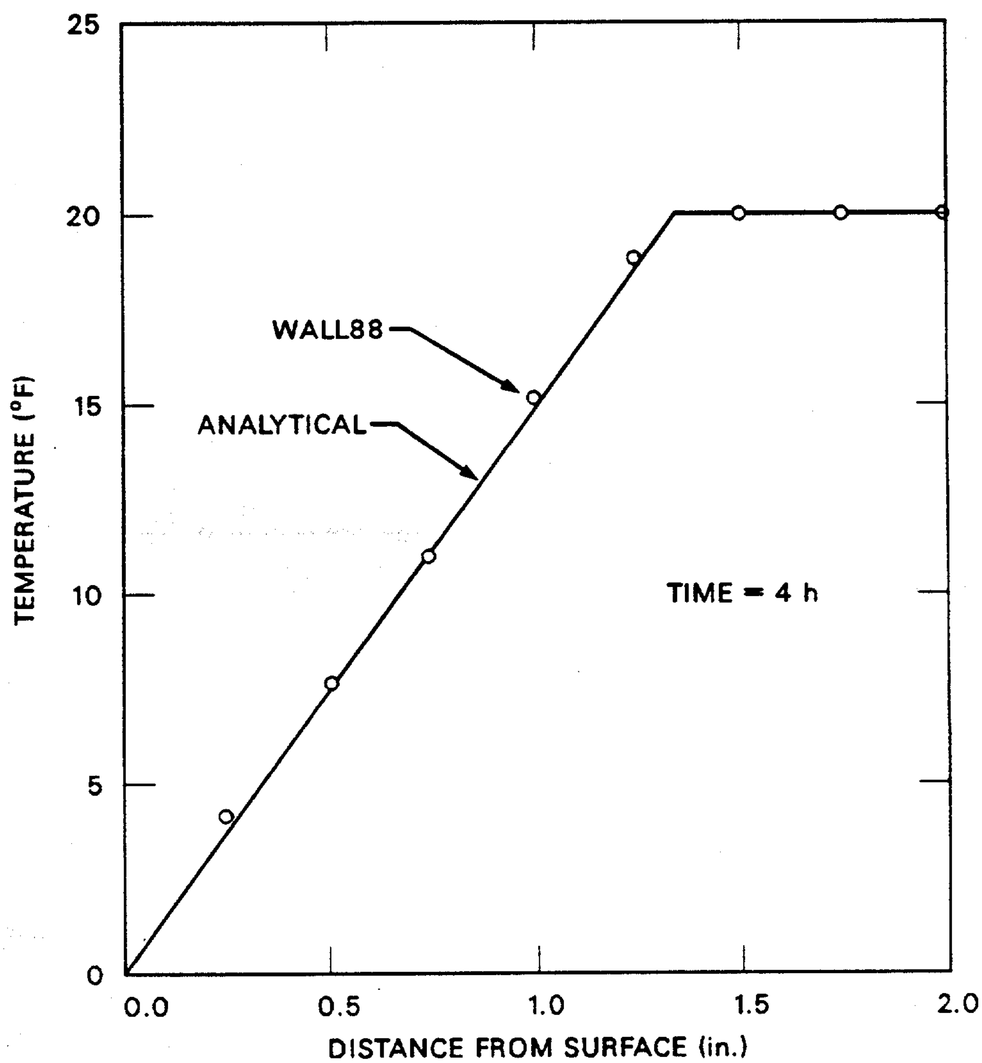

Fig. 15. Comparison of WALL88 to known analytical solution.

initial temperature would have been preferable, but the UTHA chiller capacity was insufficient to maintain constant temperatures for long periods of time below 22.2°C (72°F). The experimental data from this transient are shown in Fig. 16. Note that the entire transient lasted about 4500 min., or ~3 d. Comparatively, the transient shown in Fig. 14 at the same heater power but not including latent heat lasted only about a tenth as long. This is a good indication of the power of latent heat as an energy storage mechanism. Also shown on Fig. 16 are the results of a WALL88 simulation. For this calculation the melting point was assumed to be 23.3°C (74.0°F), which is close to the "handbook" value of 23.0°C (73.5°F). The heat of fusion of octadecane is about 195.2 kJ/kg-paraffin (84 Btu/lb-paraffin). Thus the heat of fusion of wallboard composite containing 30% paraffin would be 58.6 kJ/kg (25.2 Btu/lb) wallboard. Other parameters of the wallboard composite used in the calculation are heat capacity: 1.47 kJ/kg•°C (0.35 Btu/lb•°F), and thermal conductivity: 0.835 kJ/h•m•°C

ORNL-DWG 90C-3754R ETD

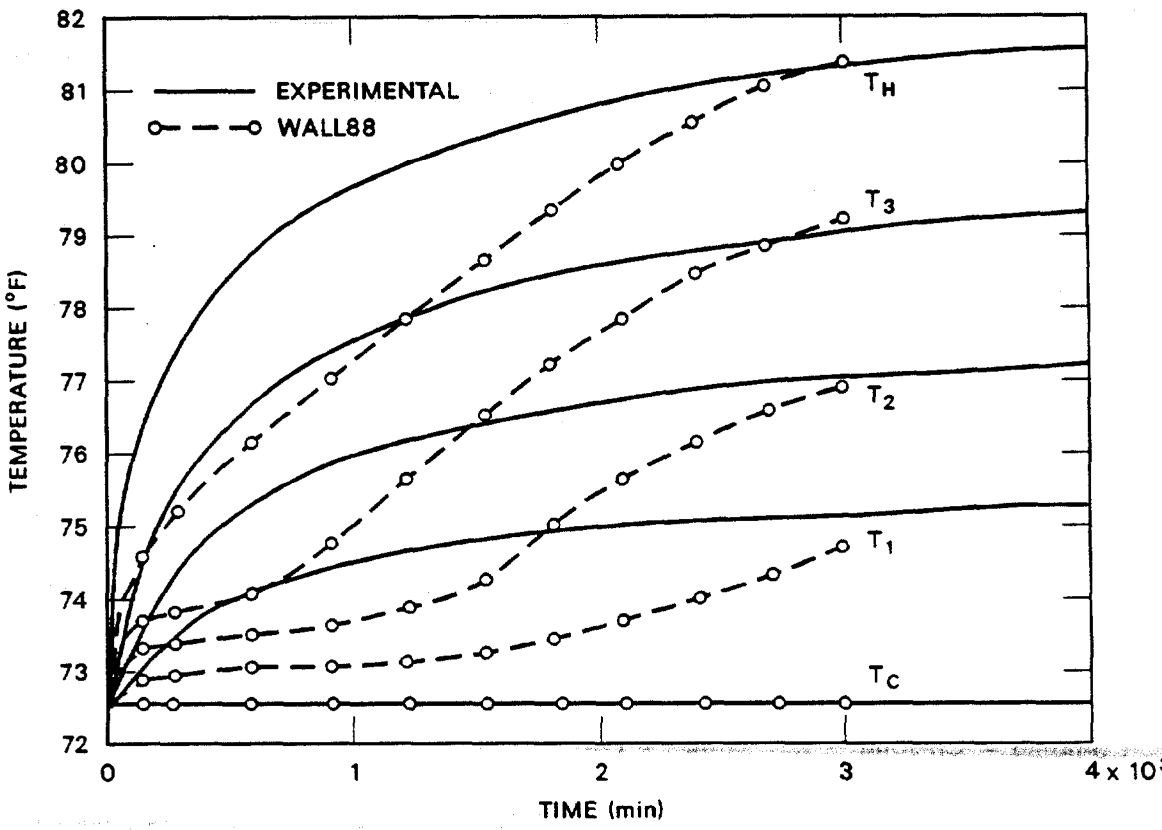

Fig. 16. Comparsion of WALL88 to experimental transient data. Assumed melting point: 74°F.

(0.134 Btu/h•ft•°F). As shown in Fig. 16, the measured and computed temperatures do not agree. An important observation is that the computed temperatures tend to level off at the melting point [23.3°C (74.0°F)], as one would expect. However, the measured values show no tendency to level off. Other computer runs were made in which various parameters were changed such as the melting point and heat of fusion. In all cases, agreement between measured and computed temperatures was poor. All computer runs showed the same leveling effect at the melting point.

Because of the way in which the computer program handles the melting process, an isothermal process was inadequate for this situation. From the DSC plots, it can be seen that octadecane melts over a range of several degrees. Figure 10 shows that melting of the material used in these tests takes place over a range of ~5.5°C (10°F). Because the range of the transient experiments is also ~5.5°C (10°F), it is obvious that this effect must be accounted for. The computer program was thus modified to incorporate a melting range. This was accomplished by replacing the heat of fusion with a triangular heat capacity relationship as shown in Fig. 17. TA and TB represent the intersection of the triangle legs with the horizontal line on a DSC melting curve, and TM represents the "melting point" and would be the peak on a DSC melting curve. TM may be located any place between TA and TB. Cp-Max is a computed value such that the shaded area under the triangle is equal to the heat of fusion of the phase change material.

The calculations were then repeated with the modified computer program and using the following parameters:

TM = 23.3°C (74.0°F) – Handbook melting point,

$$\left.\begin{array}{l}\text{TA} = 19.5°\text{C } (67.1°\text{F}) \\ \text{TB} = 25.5°\text{C } (77.9°\text{F})\end{array}\right\} \text{– Values relative to TM determined from DSC melting curve,}$$

Cp-liquid = Cp-solid = 1.47 kJ/kg•°C (0.35 Btu/lb•°F),

Cp-max = 21.0 kJ/kg•°C (5.01 Btu/lb•°F), based on heat of fusion of 58.6 kJ/kg (25.2 Btu/lb).

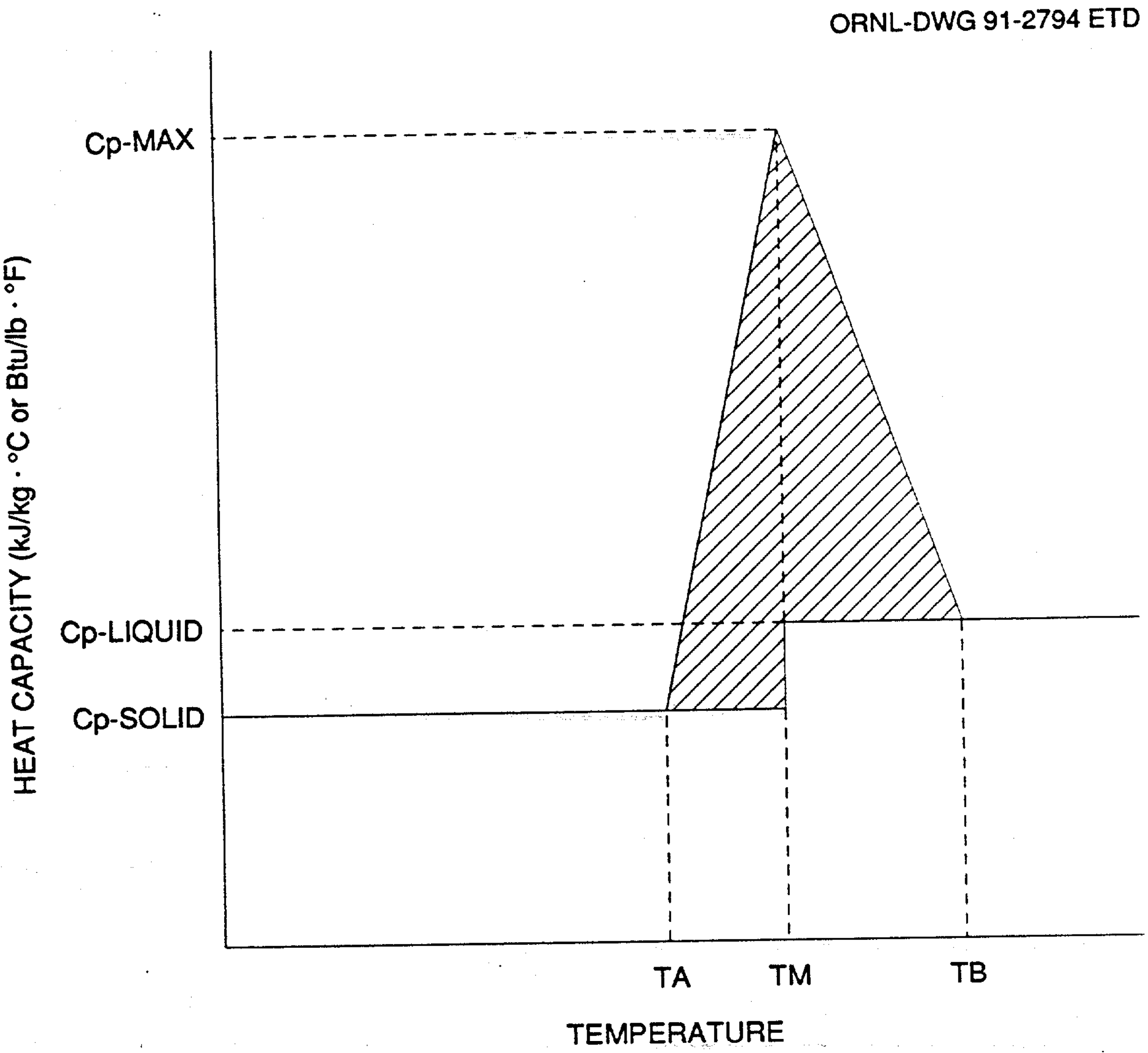

Fig. 17. Heat capacity relationship used to simulate a melting range.

The results of this change to WALL88 are shown in Fig. 18. The agreement between calculated and measured transients is better but still not good. The situation has improved mechanistically because the leveling off of the computed temperature near the paraffin melting point is no longer present.

The next computer run was based entirely on the DSC plot (Fig. 10) of the octadecane material that was used in these experiments. The value of TM was taken to be 25.8°C (78.5°F). TA and TB were taken to be the temperatures where the base of the triangular portion of the melt phase intersects the horizontal line, 22.0°C (71.6°F) and 28.0°C (82.4°F), respectively. The heat of fusion measured by the DSC includes the tail of the melt

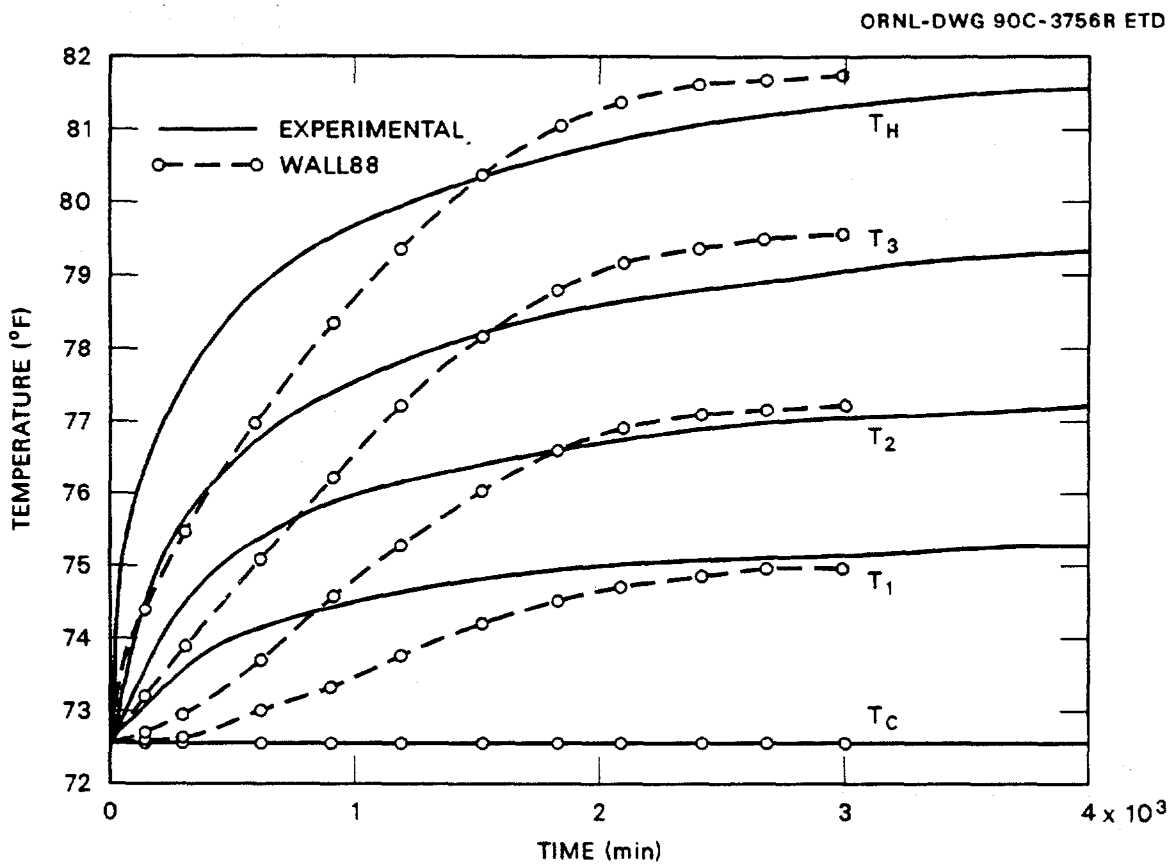

Fig. 18. Comparison of WALL88 to experimental transient data. Assumed melting parameters: TA = 67.1°F, TM = 74.0°F, TB = 77.9°F.

curve, that is, the curved portion of the melt phase between 20 and 28 min (see Fig. 10). This portion accounts for about 30% of the heat of fusion. It is not included in the triangular heat capacity relationship and it is outside the range of the transient experiment. The heat of fusion was reduced to 70% of the original value to eliminate this effect, resulting in a new value for Cp-Max of 15.2 kJ/kg•°C (3.62 Btu/lb•°F). Results of this computer run are shown in Fig. 19. The agreement between experimental and computed results has improved considerably.

The DSC plot used above to obtain melting parameters was obtained with a temperature ramp of 2°C/min (3.6°F/min). From Table 3 it can be seen that slower ramp rates result in somewhat higher melting temperatures. In addition, slower ramp rates tend to narrow the DSC peaks. For the final computer run in this series of heating transients, the value of TM was raised 0.55°C (1°F), to 26.4°C (79.5°F); the difference between TA and TB was reduced by 1.1°C (2°F). The values of TA and TB used were 23.1 and 28.0°C (73.6 and

ORNL-DWG 90C-3757R ETD

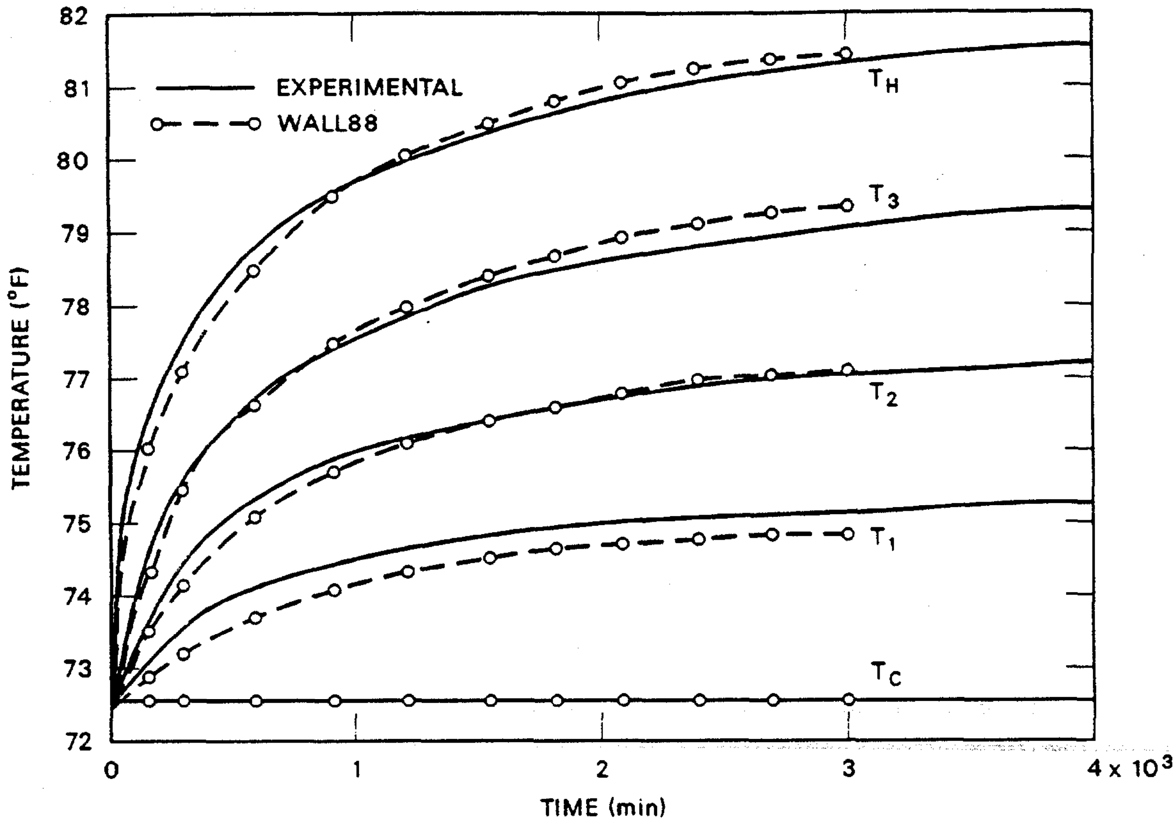

Fig. 19. Comparison of WALL88 to experimental transient data. Assumed melting parameters: TA = 71.6°F, TM = 78.5°F, TB = 82.4°F.

82.4°F), respectively. Reducing the difference between TA and TB changed the shape of the heat capacity triangular relationship; the new value for Cp-Max is 18.2 kJ/kg•°C (4.36 Btu/lb•°F). The results of this computer run are shown in Fig. 20.

Our conclusion is that either one of Figs. 19 or 20 shows that the computer model is in substantial agreement with the heating transient data. This agreement was achieved by formulating the heat of fusion into a triangular heat capacity relationship that allows the paraffin to melt over a range of temperatures. It was also necessary to assume that the paraffin melting point was the melt temperature measured by the DSC rather than the handbook melting point.

When the heating transient experiments with the UTHA had reached steady state, the electric heater was turned off. The cold plates were left on and maintained the same temperature as during the heating transient. As the stack of wallboard equilibrated to the

ORNL-DWG 90C-3758R ETD

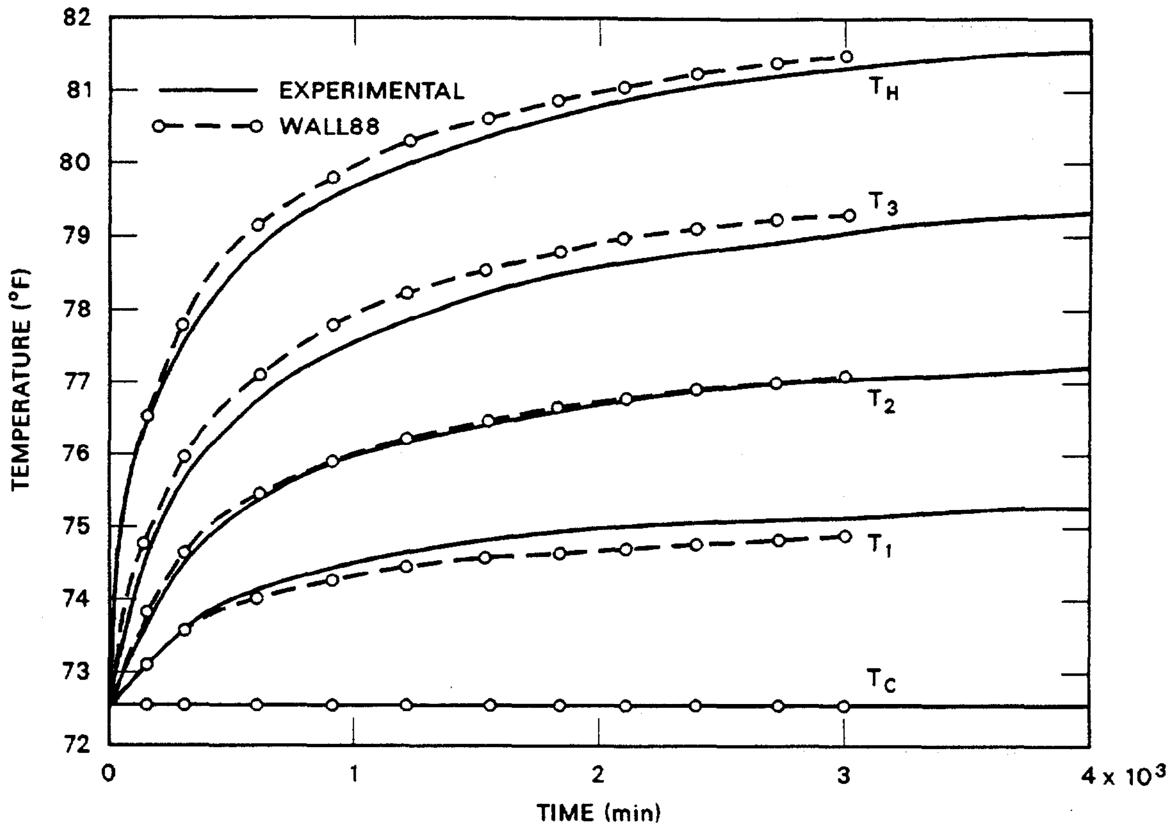

Fig. 20. Comparison of WALL88 to experimental transient data. Assumed melting parameters: TA = 73.6°F, TM = 79.5°F, TB = 82.4°F.

cold plate temperature, data for a cooling transient were generated. A series of WALL88 runs was then made in an attempt to match the computed temperatures with the measured temperatures. This series of computer runs was quite similar to the runs for the heating transient.

The data for this cooling transient are shown in Fig. 21 out to almost 4000 min. Note that temperature T_H wanders during the transient and finally ends almost 0.28°C (0.5°F) below the equilibrium temperature. The problem with TH is unknown; however, little weight will be given to this temperature in the data analysis.

The first cooling transient runs with WALL88 were conducted essentially under the same conditions as the first heating transient run. The paraffin was assumed to freeze at its handbook freezing point, in this case 23.0°C (73.5°F). All other thermal parameters (Cp, k, H_{fusion}) were taken to be the same as in the heating transient run. Results of this simulation are shown in Fig. 22. Agreement between measured and computed temperature

ORNL-DWG 90C-3759R ETD

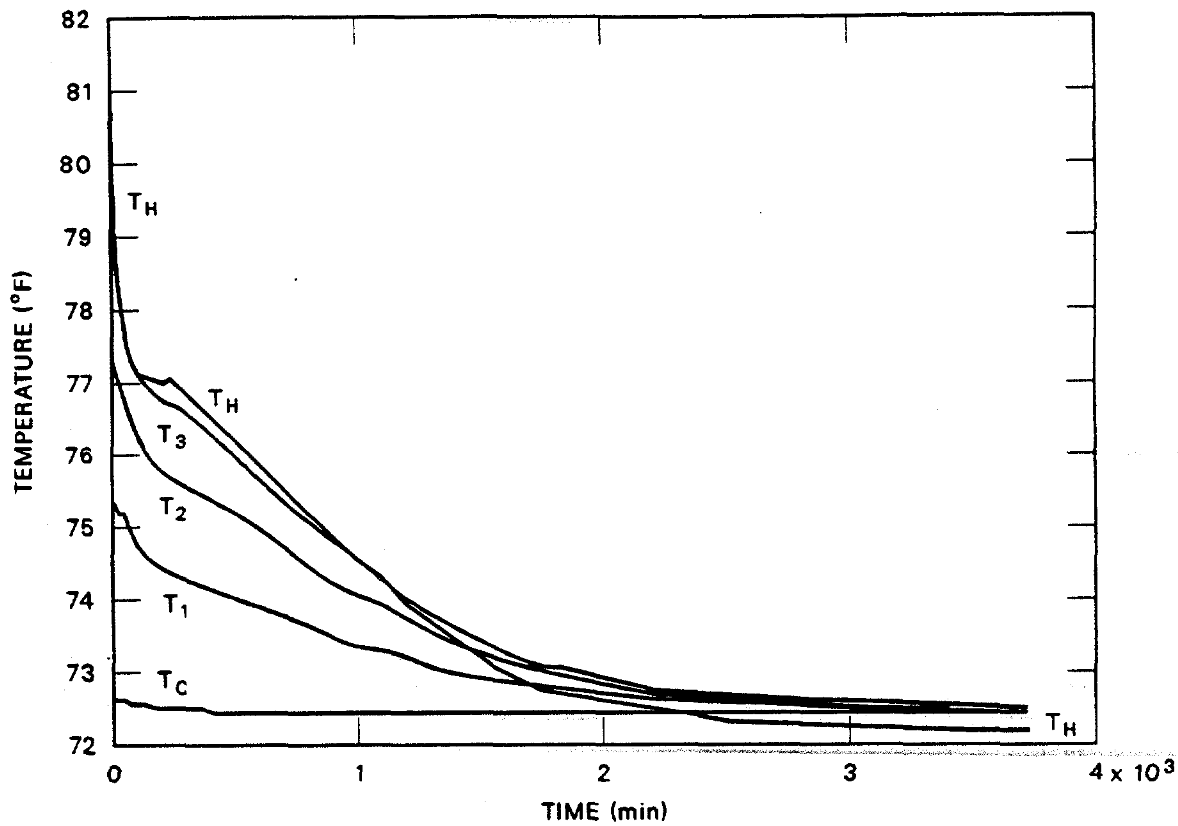

Fig. 21. Experimental cooling transient.

is very poor. Note that temperatures T_H, T_3, T_2, and T_1 decrease very quickly to the freezing point, then hold there, as would be expected. Finally, after about 600 min, T_1 starts to decrease and approach T_c. All temperatures will eventually equilibrate to T_c.

The second cooling transient run with WALL88 was similar to the second heating transient run. The triangular heat capacity relationship was used to simulate the heat of fusion. The value of TM was assumed to be the handbook freezing point, in this case 23.0°C (73.5°F); TA and TB were extrapolated from the freezing peak of the DSC plot straddle to the value of TM or 18.9 and 25.0°C (66.1 and 77.0°F), respectively. In addition, the heat of fusion of the paraffin was reduced by about 20% to remove the tail on the DSC plot. This gave a value of Cp-Max of 16.6 kJ/kg•°C (3.96 Btu/lb•°F). The results of this WALL88 run are shown in Fig. 23. The agreement between experimental and computed results has improved, but the agreement is still not good.

The third cooling transient run with WALL88 was similar to the third heating transient run. The triangular heat capacity relationship was used, and the values of its

ORNL-DWG 90C-3760R ETD

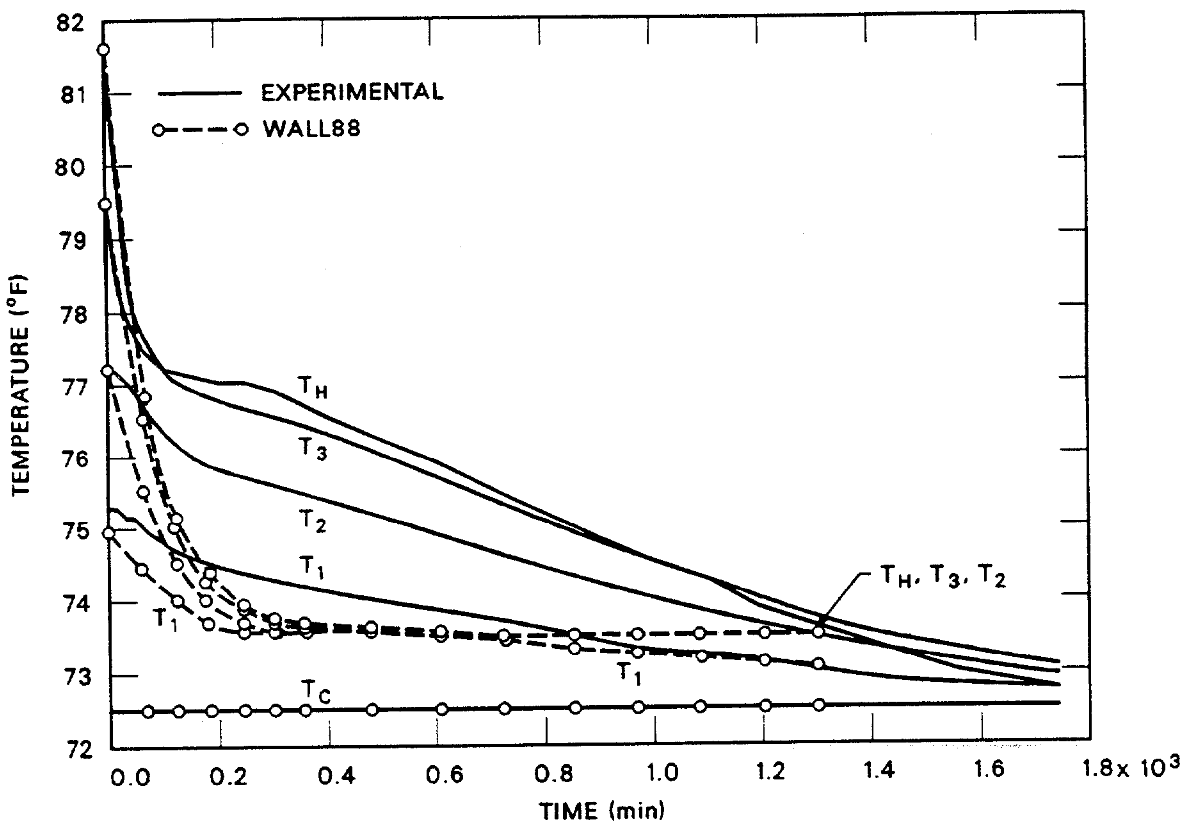

Fig. 22. Comparison of WALL88 to experiemntal transient data. Assumed freezing point: 73.5°F.

parameters taken directly from the DSC freezing curve are 16.2 and 22.3°C (61.2 and 72.1°F), respectively. TM was taken as the average of the two peak temperatures, or 20.3°C (68.6°F). Note that the entire cooling transient, which drops from a maximum of 27.5°C (81.5°F) to an isothermal temperature of 22.5°C (72.5°F), all takes place above the triangular heat capacity relationship. Good agreement is therefore not expected because sensible heat is the only thermal storage parameter involved. This plot is included for the interest of completeness. The results are shown in Fig. 24, where only the temperature next to the heater T_H is shown.

The final cooling transient run with WALL88 was based on the assumption that good agreement would be obtained by using the triangular heat capacity relationship and a freezing temperature of 23.9°C (75.0°F). TA and TB were extrapolated to this temperature and were

ORNL-DWG 90C-3761R ETD

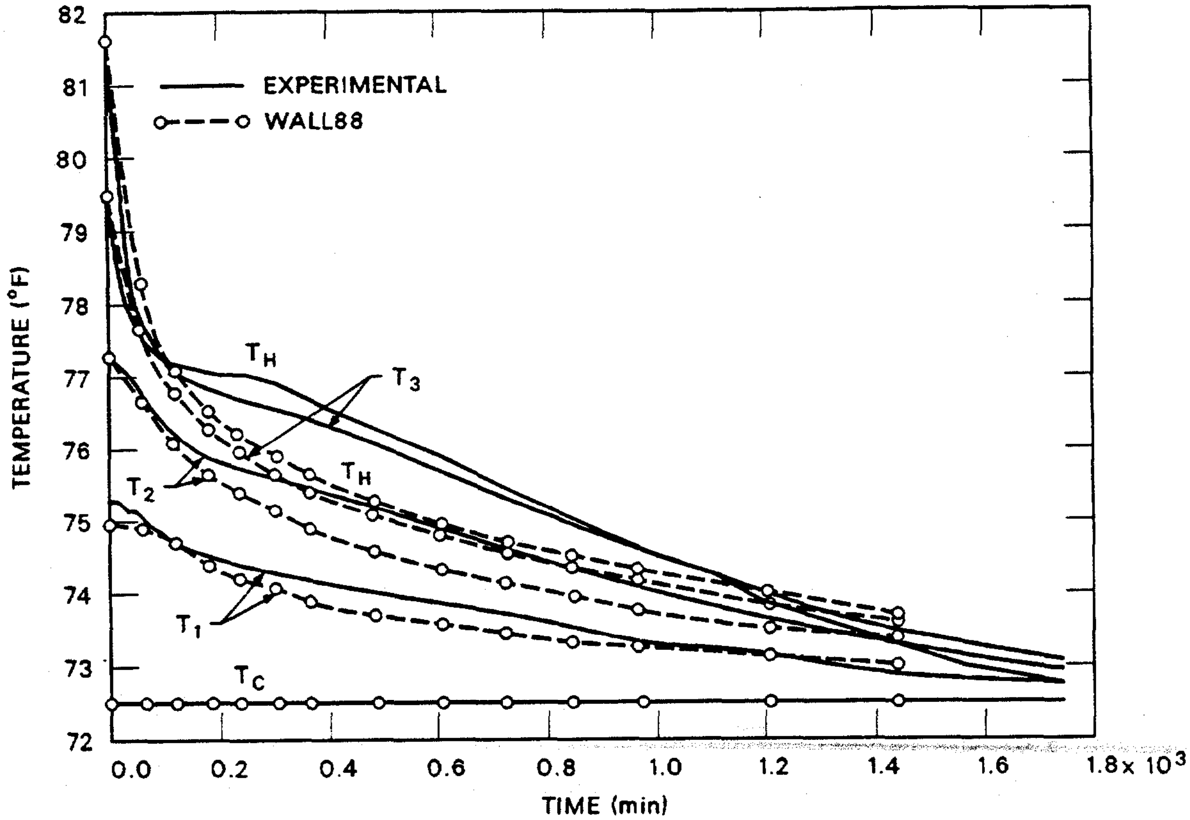

Fig. 23. Comparison of WALL88 to experimental transient data. Assumed freezing parameters: TA = 66.1°F, TM = 73.5°F, TB = 77.0°F.

estimated to be 19.8 and 25.8°C (67.6 and 78.5°F), respectively. Results of this calculation are shown in Fig. 25. The computed and experimental transient temperature profiles are in fairly good agreement although not as good as the transient heating profiles in Figs. 19 and 20. Good agreement between the computed and measured temperature was not expected for the cooling transient because of problems with the temperature recorder, and because the freezing curve on the DSC plot (Fig. 10) contains two peaks and the triangular heat capacity relationship is based on one peak. The following are a number of conclusions that can be drawn about WALL88 and the octadecane paraffin used in these thermal transient studies.

1. WALL88 was originally developed for a phase change material that melts and freezes at a specific temperature. In this form, the computer model was verified against known analytical solutions.

ORNL-DWG 90C-3762R ETD

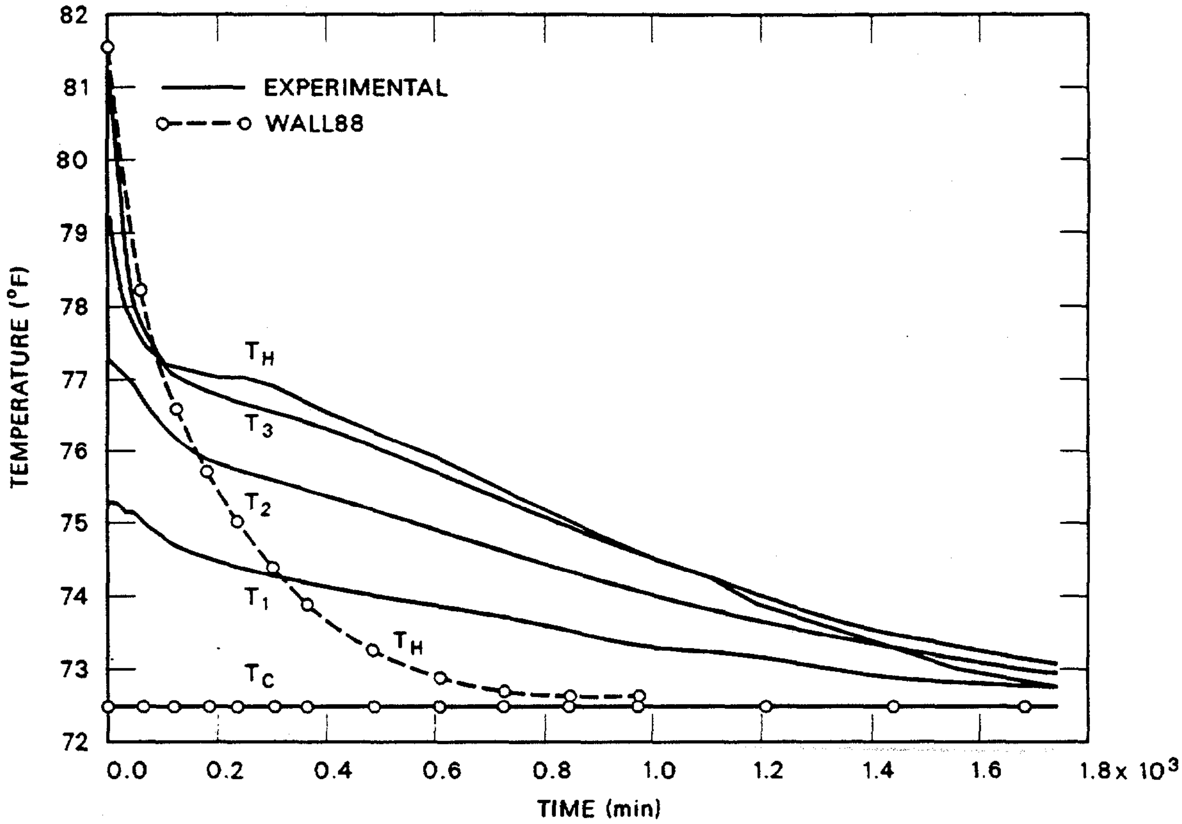

Fig. 24. Comparison of WALL88 to experimental transient data. Assumed freezing parameters: TA = 61.2°F, TM = 68.6°F, TB = 72.1°F.

2. It was necessary to modify WALL88 to obtain good agreement with experimentally generated thermal transient data with paraffin. The modification involved changing the melting point to a melting range. This was required because DSC analysis, even at very slow temperature ramps, showed that the paraffin melts and freezes over a temperature range of ~5.5°C (10°F). When this change was made, agreement between WALL88 and the heating and cooling transients was very good.
3. An unexpected result of the analysis was that the best agreement between WALL88 and transient data was obtained at a melting point of ~26.1°C (79°F) for the heating transient and ~23.9°C (75°F) for the cooling transient. This was unexpected because the paraffins are considered to be well-behaved as far as thermal performance is concerned, and melting and freezing should take place at the same temperature. There may be a valid explanation for this phenomenon. Chemists knowledgeable in the melting and freezing process contend that some materials must be "taught" how to melt and freeze.

ORNL-DWG 90C-3763R ETD

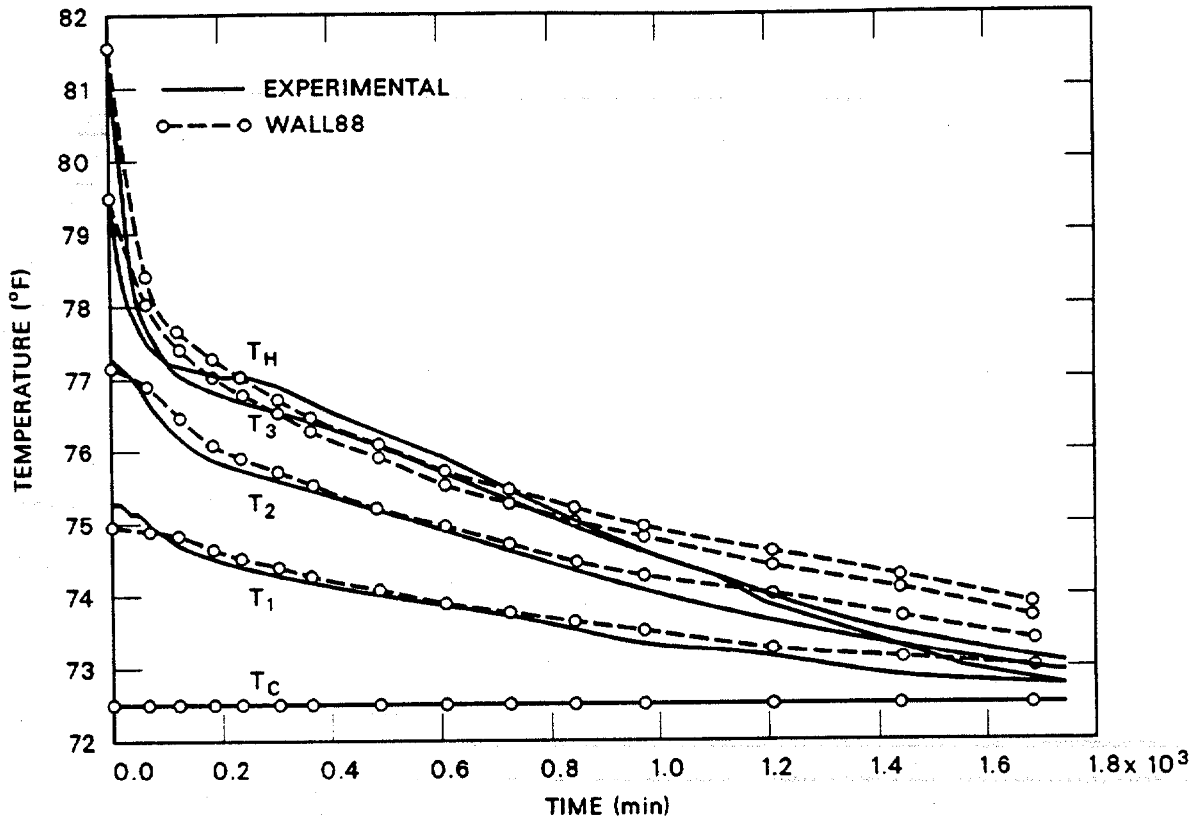

Fig. 25. Comparison of WALL88 to experimental transient data. Assumed freezing parameters: TA = 67.6°F, TM = 75.0°F, TB = 78.5°F.

This is particularly true for organic materials and when in a confined space such as the pores of wallboard. "Teaching" is accomplished by melting and freezing the material several times. For example, DSC operators often cycle materials they are testing several times before recording the data. In addition, paraffin from different sources may have different melting and freezing characteristics. Note from Table 3 that the difference between the melting and freezing temperatures for the Humphrey paraffin at 0.2°C/min is 2.9°C (5.2°F). The same temperature difference for the Witco paraffin is only about 0.055°C (0.1°F). Witco paraffin, which is obtained by fractionation of petroleum refining residues, is the cheapest source of octadecane and would therefore be the material of choice for this concept.

5. SUMMARY AND CONCLUSIONS

Conventional gypsum wallboard impregnated with octadecane paraffin has been identified by UDRI as an attractive latent heat thermal energy storage material for the passive solar application. Although there are several ways to incorporate paraffin into wallboard, simply soaking the wallboard in molten paraffin was the method of choice for this development effort. It was shown that the paraffin concentration in full-sized sheets of wallboard [1.22 by 2.44 m (4 by 8 ft)] can be controlled by the immersion time and that the paraffin distribution is uniform across the entire sheet. Approximately 160 full-size sheets were prepared for this development effort. The sheets featured wallboard by two different manufacturers, octadecane by two different manufacturing processes, wallboard of three different thicknesses (1/4, 1/2, and 5/8 in.), and three different paraffin concentrations (15, 20, and 30% by weight).

Some full-size sheets were sent to UDRI for thermal stability tests. One test consisted of maintaining several full-size sheets at an elevated temperature [37.8°C (100°F)] for an extended period of time. The results of this test are that there was no indication of paraffin redistribution within the wallboard and no loss of thermal storage capacity. A small amount of paraffin did evaporate and condense on the chamber door. This is not considered a serious problem because in the intended application the wallboard will not get as hot as in the test; the wallboard will be painted or papered to effectively stop the evaporation. The other test by UDRI consisted of thermally cycling the wallboard well above and below the paraffin melting point. This test also resulted in no discernable movement of the paraffin or loss of thermal storage capacity. An unexpected observation was the appearance of surface frost. This material looked quite similar to hoarfrost as seen on a cold winter morning. An extremely small amount of paraffin was involved, and it is easily removed. Washing the surface of the wallboard with methylethyl ketone or soapy water or painting the surface will eliminate the frosting effect. Some octadecane paraffins from different sources do not appear to frost.

A computer model, WALL88, was developed to study thermal energy transport and storage by a thermal energy storage system based on the latent heat of fusion. The model was validated by comparing it with known analytical solutions. In addition, results of the model were compared with experimentally produced thermal transients in a stack of wallboard impregnated with paraffins. To achieve good agreement between the model and experimental data, it was necessary to modify the model in such a way that the paraffin melted over a range of temperature. To accomplish this, the latent heat of fusion was replaced with a triangular-shaped heat capacity relationship that looked very similar to the triangular-shaped melting phase of a DSC curve. When this change was incorporated into the model, the agreement between computed and experimental transient data was very good.

In summary, although a few relatively minor problems were identified, no reason has thus far been discovered that would prevent the subject wallboard from being used in its intended application.

REFERENCES

1. I. O. Salyer and S. D. Donovan, "Passive Phase Change Materials for Use in Passive and Hybrid Solar Heating and Cooling Systems," in *Proceedings of the Passive and Hybrid Solar Energy Storage Update, Washington, D.C., September 26–28, 1983.*

2. I. O. Salyer et al., "Advanced Phase Change Materials for Passive Solar Storage Applications," in *Proceedings of the Passive and Hybrid Solar Energy Update, September 5–7, 1984.*

3. I. O. Salyer, A. K Sircar, and R. P. Chartoff, "Advanced Phase Change Materials for Passive Solar Storage Applications," in *Proceedings of the Solar Buildings Conference, Washington, D.C., March 18–20, 1985.*

4. I. O. Salyer et al., "Advanced Phase Change Materials for Passive Solar Storage Application, in *Proceedings of the 20th Intersociety Energy Conversions Engineering Conference, Miami Beach, Florida, August 18–23, 1985.*

5. I. O. Salyer, A. K Sircar, and R. P. Chartoff, "Analysis of Paraffinic Hydrocarbons for Thermal Energy Storage," in *Proceedings of the 15th North American Thermal Analysis Society Conference, Cincinnati, Ohio, September 12–14, 1986.*

6. I. O. Salyer, A. K. Sircar, and S. Dandiki, *Advanced Phase Change Materials and Systems for Solar Passive Heating and Cooling of Residential Buildings*, unnumbered report, University of Dayton Research Institute, Dayton, Ohio, 1988.

7. I. O. Salyer and A. K Sircar, University of Dayton Research Institute, Dayton, Ohio, *Development of Phase Change Material Wallboard*, UDR-TR-89-72, September 1989.

8. D. L. McElroy et al., "The Thermophysical Properties of Gypsum Boards Containing Wax," in *Proceedings of the 21st International Thermal Conductivity Conference, Lexington, Kentucky, October 15–18, 1989.*

9. A. Solomon, V. Alexiades, and D. G. Wilson, *The Mathematical Modeling of Melting and Freezing Processes*, Hemisphere Press (1990).

10. A. Solomon, Users Manual for WALL88 (to be published).

11. H. S. Carslaw and J. C. Jaeger, *Conduction of Heat in Solids*, Oxford University Press, London, England, 2d ed., 1959.

ORNL/TM-11541
Dist. Category UC-202

INTERNAL DISTRIBUTION

1. T. D. Anderson
2. S. H. Buechler
3. R. S. Carlsmith
4. W. G. Craddick
5. J. B. Drake
6. D. M. Eissenberg
7. W. Fulkerson
8. J. E. Jones Jr.
9. L. Jung
10. R. J. Kedl
11. M. A. Kuliasha
12. W. R. Mixon
13. M. Olszewski
14. A. E. Ruggles
15. A. C. Schaffhauser
16. M. Siman-Tov
17. T. K. Stovall
18. M. J. Taylor
19–23. J. J. Tomlinson
24. C. D. West
25. A. Zucker
26. ORNL Patent Section
27. Central Research Library
28. Document Reference Section
29–30. Laboratory Records Department
31. Laboratory Records (RC)

EXTERNAL DISTRIBUTION

32. Daniel M. Blake, Branch Manager Materials Research, Solar Energy Research Institute, 1617 Cole Blvd., Golden, CO 80401
33. S. R. Bull, Solar Energy Institute, 1536 Cole Blvd., Golden, CO 80401
34. Kevin Drost, Battelle Pacific Northwest Laboratories, P.O. Box 999, Battelle Blvd., Richland, WA 99352
35. Russ Eaton, Advanced Utility Concepts Division, U.S. Department of Energy, Forrestal Bldg., CE-142, 1000 Independence Ave., Washington, DC 20585
36. Ronald S. Finkelstein, Gold Bond Building Products, Research Center, 1650 Military Road, Buffalo, NY 14327
37. D. E. Gound, Program Manager, Research Management Branch, Department of Energy, ORO, P.O. Box 2001, Oak Ridge, TN 37831-8611
38. Lloyd Huff, Associate Director of Special Projects, The University of Dayton, 300 College Park, Dayton, OH 45469-0001
39. Landis Kannberg, Battelle Pacific Northwest Laboratories, P.O. Box 999, Battelle Blvd., Richland, WA 99352
40. Larry W. Kingston, Research Center, Gold Bond Building Products, 1650 Military Road, Buffalo, NY 14217-1198
41. Kurt W. Klunder, Director, Office of Energy Management, Office of Utility Technology, U.S. Department of Energy, CE-14, Forrestal Bldg., 1000 Independence Ave., Washington, DC 20585

42. George Manthey, Department of Energy, ORO, P.O. Box 2001, Oak Ridge, TN 37831
43. Don Neeper, Advanced Engineering Technology Group, Los Alamos National Laboratory, MS J576, Los Alamos, NM 87545
44. Veronica A. Rabl, Electric Power Research Institute, 3412 Hillview Ave., P.O. Box 10412, Palo Alto, CA 94303
45. Eberhart Reimers, Advanced Utility Concepts Division, U.S. Department of Energy, Forrestal Bldg., CE-142, 1000 Independence Ave., Washington, DC 20585
46. Ival O. Salyer, University of Dayton Research Institute, 300 College Park, Dayton, OH 45469-0001
47. Robert L. San Martin, Deputy Assistant Secretary, Office of Utility Technology, U.S. Department of Energy, Forrestal Bldg., CE-10, 1000 Independence Ave., Washington, DC 20585
48. Paul Shipp, U.S. Gypsum Corporation, Research Center, 700 N. Highway 45, Libertyville, IL 60048
49. Ronald D. Wendland, Project Manager, Thermal Storage Technology, P.O. Box 10412, 3412 Hillview Ave., Palo Alto, CA 94303
50. Office of Assistant Manager for Energy Research and Development, Department of Energy, ORO, Oak Ridge, TN 37831

51–62. Given distribution as shown in DOE/OSTI-4500-R75 under category UC-202 (Thermal Energy Storage)